



## **Increased Protein and Transcript Expression Levels of Lysine-Specific Demethylase 1 (LSD1) Signify Worse Prognosis in Triple-Negative Breast Cancer**

Dong Yeul LEE<sup>1,2</sup>, Bennett LEE<sup>3,4</sup>, Stefano PERNA<sup>4</sup>, Johnathan Xiande LIM<sup>1</sup>, Joe Poh Sheng YEONG<sup>1,5</sup>, Puay Hoon TAN<sup>1,6</sup>, Javed IQBAL<sup>1,6</sup>

<sup>1</sup>- Singapore General Hospital, Department of Anatomical Pathology, Singapore. 20 College Road, Academia, Level 10, Diagnostics Tower, Histopathology Laboratory, Department of Anatomical Pathology, Singapore 169856

<sup>2</sup>- Nanyang Technological University, School of Biological Sciences, Singapore. 60 Nanyang Dr, Singapore 637551

<sup>3</sup>- Agency of Science, Technology and Research (A\*STAR), Singapore Immunology Network (SIgN), Singapore. 8A Biomedical Grove Level 3 & 4. Immunos Building Singapore 138648

<sup>4</sup>- Nanyang Technological University, Centre of Biomedical Informatics, Singapore. 59 Nanyang Dr, Singapore 636921

<sup>5</sup>- Agency of Science, Technology and Research (A\*STAR), Institute of Molecular Cell Biology (IMCB), Singapore. 61 Biopolis Dr, Singapore 138673

<sup>6</sup>- Duke-NUS Medical School, Singapore. 8 College Rd, Singapore 169857

Corresponding Author: Dr Javed Iqbal

Email: [javed.iqbal@singhealth.com.sg](mailto:javed.iqbal@singhealth.com.sg)

Address: Department of Anatomical Pathology, Singapore General Hospital, 20 College Road, Academia, Level 10, Diagnostics Tower, Singapore 169856

## ABSTRACT

Epigenetic alterations can lead to altered gene functions and cellular neoplastic transformation, contributing to cancer initiation and progression. Lysine-specific demethylase 1 (LSD1), the first identified histone demethylase in 2004, has increasingly been shown to be overexpressed in various cancers and to regulate carcinogenesis. Thus, this study aims to investigate the effects of LSD1 protein and transcript in triple-negative breast cancer (TNBC) while evaluating its association with clinicopathological parameters and survival outcomes.

A total of 389 TNBC cases diagnosed at the Department of Anatomical Pathology, Singapore General Hospital from 2003 to 2014 were used. Tissue microarrays were constructed, and immunohistochemistry was performed using an antibody against LSD1. LSD1 transcript (*KDM1A*) levels and their association with survival outcomes were assessed in three cohorts (METABRIC, TCGA, FUSCC). Differentially expressed genes (DEGs) between the LSD1 and *KDM1A* sample groups were identified using Welch's t-tests with multiple testing corrections.

A total of 80.7% of TNBC patients expressed LSD1 protein, which was significantly associated with shorter overall survival ( $P = 0.036$ ). Four genes (*ELOC*, *COPS5*, *MTDH*, *VEGFR1*) were further revealed to be upregulated in LSD1+ TNBCs, while a higher *COPS5* and *ELOC* expression was found to be significantly associated with worse OS. Increased *KDM1A* levels were additionally associated with worse disease-free survival ( $P = 0.019$ ) in TCGA. A total of 2135 overlapping genes were found to be differentially expressed between *KDM1A* high-low TNBCs, with significantly enriched functions involved in cell proliferation pathways (cell cycle, DNA replication).

Our results support the prognostic significance of increased LSD1 protein expression to be associated with poorer survival in TNBC patients. The identification of both LSD1/*KDM1A*-associated DEGs and their key relationship with oncogenic pathways further support aberrant LSD1 epigenetic expression in influencing TNBC heterogeneity. Overall, the study warrants the role of LSD1 as a potential TNBC target.

## INTRODUCTION

Triple-negative breast cancer (TNBC) is an aggressive breast cancer subtype defined by the lack of estrogen receptor (ER), progesterone receptor (PR) and human epidermal growth factor receptor 2 (HER2) expression [1]. TNBC represents approximately 10-20% of diagnosed breast cancers that occur mostly in premenopausal young women (under 40 years old). TNBC can be further stratified based on the mRNA levels of different genes to decipher and accurately predict prognosis improvements in TNBC heterogeneity [2]. Despite this, molecular profiling remains limited in routine clinical practice due to high costs, and the identification of other potential surrogate predictors of outcomes is necessary. While epigenetic modification has been previously established to be involved in normal development functions [3], aberrant epigenetic modifications are increasingly recognized in different malignancies, including breast cancer [4]. Epigenetic modifications (including histone modifications) precede genetic changes, occur at the early onset of neoplastic development, and can cause altered gene function and cellular neoplastic transformation [5]. Thus, advancements in understanding the epigenetic machinery may help identify which mechanisms drive TNBC aggressiveness. Considering that limited therapeutic targets currently exist for TNBC subtypes, there is an increasing interest in investigating epigenetic modifications and their implications for breast cancer pathogenicity, biomarkers, prevention and treatment [4].

Lysine-specific demethylase 1 (LSD1) encodes a nuclear protein that contains 3 domains: SWIRM, Tower, and amine oxidase-like [6]. LSD1 allows transcription factors or corepressor complexes to activate or repress transcription through its role in targeting mono- or di-methylated histone H3K4 and H3K9, as well as nonhistone substrates. The target specificity of LSD1 with several partners enables the formation of different complexes that regulate gene expression [7]. Increased levels of LSD1 were observed in ER(-) breast cancers [8], along with an inverse correlation between its expression and low PR status [9]. Overexpression of LSD1 is reportedly significantly associated with shorter relapse-free survival (RFS) in TNBC and poorer prognosis in the basal-like phenotype [10], where it is implicated in facilitating breast cancer disease [11]. The LSD1 transcript (referred to as *KDM1A* hereafter), is an essential gene involved in crucial cellular roles (normal hematopoiesis, neuronal stem cells, cancer stem cell regulation) of various tumors [12]. Cancer stem cells (CSCs) in TNBC have previously shown higher *KDM1A* expression, where the therapeutic utility of *KDM1A* inhibitors effectively reduced sphere formation and the self-renewal ability of CSCs [13]. Additionally, a clinically-used LSD1/*KDM1A* inhibitor (ORY-1001) has recently been proven to inhibit proliferation and promote apoptosis in TNBC cells, accompanied by altered proliferation and apoptosis-related protein expression [14] – featuring an effective therapeutic target in reducing stemness and TNBC disease progression. Notably, LSD1 inactivation also promotes intratumoral CD8+ T cell expansion and antitumor immunity, highlighting an important avenue to exploit LSD1 for enhanced persistence of cytotoxic T cells in cancer immunotherapies [15-17]. While many findings generally suggest a tumor-promoting role for LSD1 in breast cancers, the detailed LSD1 mechanistic role and how it is upregulated in contributing to the neoplastic conversion of TNBCs remain elusive. Therefore, our study aimed to investigate the impact of both LSD1 protein and transcript expression in a larger subset of TNBC patients to elucidate its potential role as a prognostic marker and therapeutic target.

## **METHODS**

### **Study Design and Clinicopathological Parameters**

A total of 389 archival formalin-fixed paraffin-embedded (FFPE) TNBC patient specimens diagnosed between 2003 and 2014 at the Department of Anatomical Pathology, Division of Pathology, Singapore General Hospital (SGH) were analysed. Fifty-two cases were excluded due to depleted tumor regions and/or IHC staining artifacts. All samples were obtained before patients underwent chemotherapy or radiotherapy; receipt of neoadjuvant therapy was an exclusion criterion.

### **Tissue microarray (TMA) construction**

Tumor regions for TMA construction were selected based on pathological assessment of >50% of the sample being tumor area. For each sample, two or three representative tumor cores of 1 mm diameter were transferred from donor FFPE tissue blocks to recipient TMA blocks using an MTA-1 Manual Tissue Arrayer (Beecher Instruments, Sun Prairie, WI, USA). TMAs were constructed as previously described [18].

### **Immunohistochemistry (IHC) analysis of TMAs**

TMA sections of 4  $\mu$ m thickness were incubated with antibodies specific for LSD1 (clone 1B2E5). Details of the LSD1 antibody, labeling patterns, controls, and dilution factors are listed in **Supplementary Table 1**. Scoring of antibody-labeled sections was carried out for nuclear LSD1 positivity. To generate the score, images of the labeled slides were captured using an IntelliSite Ultra-Fast Scanner (Phillips, Eindhoven, Netherlands) before independent scoring by two trained pathologists blinded to the clinicopathological and survival information. Immunoscoring was performed to determine the staining intensity and percentage of tumor cells stained in each TMA core. Where discordant, the cases were reviewed, and a consensus score was given.

The H-score for LSD1 expression in each TMA was scored and calculated as follows: (3 x % of strong and complete nuclear staining in >30% of tumor cells) + (2 x % of moderate and complete nuclear staining in >10% of tumor cells) + (1 x % of faint/weak nuclear staining in <10% of tumor cells). H-score of  $\geq 2.5$  (20% percentile cutoff) for LSD1 nuclear staining was categorized as positive, and tumors were divided into “LSD1 positive” and “LSD1 negative” subsets.

### **RNA extraction and NanoString gene expression measurement**

RNA was extracted from unlabeled FFPE sections of 10  $\mu$ m thickness using the RNeasy FFPE kit (Qiagen, Hilden, Germany) on a QIAcube automated sample preparation system (Qiagen, Hilden, Germany) and was quantified by an Agilent 2100 Bioanalyzer system (Agilent, Santa Clara, CA, USA). A total of 100 ng functional RNA (>300 nucleotides) was assayed on the nCounter MAX Analysis System (NanoString Technologies, Seattle, WA, USA). The NanoString counts were normalized using positive control probes and housekeeping genes, as previously reported [19]. The count data were then logarithmically transformed prior to further analysis. A total panel of 879 hypoxia-, immune- and cancer-associated genes was tested for significant differences between sample groups.

### **KEGG pathway enrichment analysis**

Kyoto Encyclopedia of Genes and Genomes (KEGG) pathway enrichment analysis was conducted in the Database for Annotation, Visualization, and Integrated Discovery (<https://david.ncifcrf.gov/home.jsp>) [20, 21] under *Homo sapiens* species selection. Statistical significance was defined by an FDR corrected value < 0.05.

### **Establishment of interactive network, modules and hub genes**

The Search Tool for the Retrieval of Interacting Genes/Proteins (STRING v11.5) (<https://string-db.org/>) integrates information between known and predicted protein-protein interactions (PPIs) from multiple species [22]. PPI networks were constructed using both STRING (interaction score of 0.4, FDR stringency of 5%) and Cytoscape v3.9.0 (<https://cytoscape.org/>) [23] to visualize the relationship between genes. To characterize hub genes within the network, the cytoHubba plugin v0.1 [24] was used to calculate node scores, and the nodes were ranked based on degree.

### **Follow-up and statistical analysis**

Follow-up data were obtained from medical records. DFS and OS were defined as the time from diagnosis to recurrence or death/date of last follow-up, respectively. Statistical analysis was performed using RStudio running R version 4.0.3 ([www.r-project.org](http://www.r-project.org)). Survival outcomes were estimated with the Kaplan-Meier method and compared between groups using log-rank statistics. The correlation between two variables was analyzed using Spearman's tests, where significant differences between two groups were analyzed by two-tailed tests. All genomic survival data for breast cancer patients (with "PR", "ER" and "HER2" negative expression) were obtained from various publicly available databases. Data for the Molecular Taxonomy of Breast Cancer International Consortium (METABRIC) and The Cancer Genome Atlas (TCGA) were obtained from cBioPortal (<https://www.cbioportal.org/>) [25, 26]. Data for Fudan University Shanghai Cancer Center (FUSCC) were obtained from BioSino (<https://www.biosino.org/node/>) under project ID OEP000155 [27], and the updated profiling files were obtained from the Fudan Data Portal for Cancer Genomics ([http://fudan-pgx.3steps.cn/cdataportal/study/summary?id=FUSCC\\_BRCA\\_2022](http://fudan-pgx.3steps.cn/cdataportal/study/summary?id=FUSCC_BRCA_2022)) [28].

Differentially expressed genes (DEGs) between sample groups were identified using Student's t-tests with Welch's correction. Multiple testing bias was adjusted using the Benjamini-Hochberg correction. Prognostic models were compared using ANOVA to evaluate the delta in the log-likelihood of the models ( $\Delta LR_{X^2}$ ). Statistical significance was defined by a P value < 0.05.

## **RESULTS**

### **Positive LSD1 nuclear staining is significantly associated with poorer overall survival in TNBC patients**

LSD1<sup>+</sup> nuclear staining in tumor cells was present in approximately 80.7% (272/337) of TNBC patients (**Figure 1A**). LSD1<sup>+</sup> TNBC patients reported significantly poorer overall survival (OS:  $P = 0.036$ ) (**Figure 1C**) and a consistent trend toward poorer disease-free survival (DFS:  $P = 0.269$ ) (**Figure 1B**).

### **Increased positive LSD1 expression is observed in higher lymph node status and Malay ethnic groups**

The LSD1 expression level was evaluated with respect to different clinicopathological features (age group, histological grade, lymph node status, race, tumor size) (**Figure 2**,

**Supplementary Table 2A**). Interestingly, increased LSD1 positivity was reported in TNBC patients with higher lymph node status (1 vs. 3,  $P = 0.04$ ) and Malay ethnicity (Chinese vs. Malay,  $P = 0.04$ ; Indian vs. Malay,  $P = 0.02$ ) (**Figure 2C-D**). While the younger age group, higher histological grade and larger tumor size denoted a trend toward increased LSD1 expression, no statistical significance was observed.

### **Identification of key differentially expressed genes in LSD1-positive TNBCs**

Within LSD1-expressing TNBC samples, quantifiable NanoString RNA gene panel of 879 hypoxia-, immune- and cancer-associated genes were evaluated. Subsequently, Student's t-tests with Welch correction revealed four genes with significant differential expression (**Figure 3A, Supplementary Table 3**). LSD1+ TNBC sample groups presented markedly higher gene expression (of *COPS5*, *ELOC*, *MTDH*, *VEGFR1*) than LSD1- TNBCs (**Figure 3B-E**). Moreover, TNBCs with higher *COPS5* and *ELOC* expression were found to be significantly associated with worse OS (**Figure 3F-G**), while higher *MTDH* expression showed a consistent tendency toward poorer OS (**Figure 3H**). Conversely, while patients with higher *VEGFR1* expression presented a better prognostic trend (**Figure 3I**), statistical significance was not achieved. Among the four LSD1-associated DEGs, three (*COPS5*, *ELOC*, *MTDH*) presented the most similarly clustered gene expression profile within the TNBC cohort (**Figure 4**).

### **LSD1 nuclear expression and its associated DEGs add significant prognostic power to classical clinicopathological parameters**

To further demonstrate the prognostic power of LSD1, we examined the impact of LSD1 and its associated DEGs on survival outcome analysis with a panel of typical clinicopathological features (patient age at diagnosis, tumor grade, tumor size 20 mm, lymph node status) (**Table 1**). As shown, the addition of LSD1 nuclear staining alone to clinicopathological features significantly increased the prognostic value for OS ( $\Delta LR_{\chi^2} = 1.80$ ,  $P = 1.56e-09$ ). Similarly, the inclusion of individual DEGs (*COPS5*, *ELOC*, *MTDH*) similarly increased the prognostic value for OS ([*COPS5*:  $\Delta LR_{\chi^2} = 0.38$ ,  $P = 5.24e-09$ ][*ELOC*:  $\Delta LR_{\chi^2} = 0.61$ ,  $P = 4.21e-09$ ]) and DFS ([*MTDH*:  $\Delta LR_{\chi^2} = 0.75$ ,  $P = 5.63e-06$ ]).

Of interest, the prognostic power of added DEGs into the derived LSD1-prognostic model was examined (**Table 2**). Notably, for OS alone, the inclusion of key DEGs into the existing LSD1 prognostic model further conferred an improved prognostic value ([*COPS5*:  $\Delta LR_{\chi^2} = 0.34$ ,  $P = 1.24e-08$ ][*ELOC*:  $\Delta LR_{\chi^2} = 0.35$ ,  $P = 1.23e-08$ ]).

### **Higher *KDM1A* gene expression is associated with poorer survival, younger age, elevated Ki67 levels, black or African-American ethnicity, basal and BLIS molecular subtypes**

The association between *KDM1A* gene expression and survival outcomes was evaluated using three public breast cancer cohorts (TCGA, METABRIC, FUSCC) (**Figure 5**). In TCGA, TNBC patients with higher *KDM1A* expression reported significantly worse DFS ( $P = 0.01852$ ) (**Figure 5A**). While higher *KDM1A* expression observed a consistently poorer survival trend across other TNBC cohorts, statistical significance was not achieved in their case.

Within the same TNBC cohort, transcript levels between different clinicopathological features were assessed (**Figure 6, Supplementary Table 2B-D**). In TCGA, higher *KDM1A* expression was observed in patients of black or African-American ethnicity (black or

African-American vs. white,  $P < 0.001$ ) (**Figure 6B**). In METABRIC, higher *KDM1A* expression was observed in the basal subtype (basal vs. claudin-low,  $P < 0.001$ ); basal vs. Her2,  $P < 0.001$ ; basal vs. LumA,  $P = 0.02$ ; basal vs. normal,  $P = 0.02$ ) (**Figure 6E**). In FUSCC, higher *KDM1A* expression was observed in younger age (below median age vs. equal or above median age,  $P < 0.01$ ) (**Figure 6F**), basal subtype (basal vs. other,  $P < 0.001$ ) (**Figure 6G**), elevated Ki67 levels (below Ki67 median vs. equal or above Ki67 median) (**Figure 6H**) and BLIS molecular subtype (BLIS vs. IM,  $P < 0.001$ ; BLIS vs. LAR,  $P < 0.001$ ; BLIS vs. MES,  $P < 0.001$ ) (**Figure 6I**).

### **Identification of overlapping DEGs in *KDM1A* high-low TNBCs**

Within TCGA TNBC samples with 17,213 quantifiable gene data, Student's t-test with Welch correction revealed 1 gene with significant differential expression (**Figure 7A**). Within METABRIC TNBC samples with 24,368 quantifiable gene data, Student's t-test with Welch correction revealed 6056 genes with significant differential expression (**Figure 7B**). Within FUSCC TNBC samples with 45,308 quantifiable gene data, Student's t-test with Welch correction revealed 6524 genes with significant differential expression (**Figure 7C**). In summary, significant overlapping DEGs within *KDM1A* high-low TNBCs across 3 cohorts are visualized in **Figure 7D**: 2134 genes were found to overlap between FUSCC and METABRIC, and 1 gene was found to overlap between all 3 cohorts.

To ascertain the affected pathways of 2135 overlapping DEGs within *KDM1A* high-low TNBCs, KEGG pathway analysis revealed significantly enriched terms involved in the cell cycle and DNA replication (**Figure 7E**, **Supplementary Table 4**).

### **PPI network of dysregulated cell cycle-related genes in *KDM1A*<sup>high</sup> TNBCs**

To identify key cell cycle modulatory genes in *KDM1A*-expressing TNBCs, a PPI network was constructed to estimate the interaction relationship between the 55 cell cycle genes: 55 nodes and 914 edges were used (**Figure 8A**).

Subsequently, the top 10 hub genes (by degree) of the network were identified and sequentially ranked (from 1 to 10) as follows: cyclin-dependent kinase 1 (*CDK1*), cyclin B1 (*CCNB1*), cell division cycle 20 (*CDC20*), cyclin-dependent kinase 2 (*CDK2*), cyclin A2 (*CCNA2*), cyclin B2 (*CCNB2*), cell division cycle 6 (*CDC6*), checkpoint kinase 1 (*CHEK1*), polo-like kinase 1 (*PLK1*), and minichromosome maintenance complex component 7 (*MCM7*), as shown in **Figure 8B**. Furthermore, *KDM1A*<sup>high</sup>-expressing TNBC sample groups presented markedly higher cell cycle-associated hub gene expression (*CDK1*, *CCNB1*, *CDC20*, *CDK2*, *CCNA2*, *CCNB2*, *CDC6*, *CHEK1*, *PLK1*, *MCM7*) than *KDM1A*<sup>low</sup> TNBCs (**Figure 8C-L**, **Supplementary Table 5**).

### **Prognostic value of cell-cycle hub genes in the TNBC cohort**

To evaluate the prognostic value of significantly upregulated cell cycle-associated hub genes in *KDM1A*<sup>high</sup>-expressing TNBCs, comparative survival analysis of different cohorts was performed (**Table 3**, **Supplementary Figure 1**). Within the 10 cell cycle-associated genes, higher expression in two genes (*CDC6*, *PLK1*) noted significantly poorer TNBC survival rates (**Supplementary Figure 1G and 1I**).

### **LSD1/*KDM1A*-expressing TNBCs inversely correlate with immune activity signature**

To characterize LSD1 protein or transcript expression and its correlation with the degree of immune response activation within tumors, Spearman's test was conducted in all TNBC cohorts. An immune gene set previously demonstrated to predict effective antitumor response

upon LSD1 inhibition was used (*CCL5*, *CCR5*, *CXCL9*, *CXCL10*, *CXCR3*, *CD3*, *CD4*, *CD8*, *CD274/PD-L1*, *IFNG*, *IFNGR1*, *IFNGR2*). Among immune-related genes, both LSD1-prognostic DEGs (*COPS5*, *ELOC*) and LSD1 mRNA appears to be consistently negatively correlated with CD3 ([SGH: *COPS5* vs *CD3D* = -0.21, *ELOC* vs *CD3D* = -0.19], [METABRIC: *KDM1A* vs *CD3D* = -0.16, *KDM1A* vs *CD3E* = -0.07, *KDM1A* vs *CD3G* = -0.10], [FUSCC: *KDM1A* vs *CD3D* = -0.24, *KDM1A* vs *CD3E* = -0.20, *KDM1A* vs *CD3G* = -0.21], [TCGA: *KDM1A* vs *CD3D* = -0.18, *KDM1A* vs *CD3E* = -0.22, *KDM1A* vs *CD3G* = -0.25]), CD4 ([SGH: *COPS5* vs *CD4* = -0.19, *ELOC* vs *CD4* = -0.12], [METABRIC: *KDM1A* vs *CD4* = -0.22], [FUSCC: *KDM1A* vs *CD4* = -0.28], [TCGA: *KDM1A* vs *CD4* = -0.34]), and CD8 ([SGH: *COPS5* vs *CD8A* = -0.21, *COPS5* vs *CD8B* = -0.25], [METABRIC: *KDM1A* vs *CD8A* = -0.12, *KDM1A* vs *CD8B* = -0.18], [FUSCC: *KDM1A* vs *CD8A* = -0.16, *KDM1A* vs *CD8B* = -0.10], [TCGA: *KDM1A* vs *CD8B* = -0.27]) in aggressive TNBCs (**Figure 11, Table 4**).

## DISCUSSION

In this study, we investigated the role of increased LSD1 activity in TNBC tumors. LSD1 is known to promote cell proliferation [29] with observed sublocalization changes and reduced H3K4 monomethylation levels in the early response to chemical carcinogens [30], suggesting LSD1's capacity to influence multiple genes critical for mammary carcinogenesis. High LSD1 expression has been proven to be a biomarker for aggressive tumor biology and histological grading in hormone receptor-negative breast cancers [8], ductal carcinoma *in situ* and infiltrative ductal carcinomas [9]. With limited ongoing clinical studies validating the significance of LSD1 expression in TNBCs [10, 31], our study aimed to evaluate the clinical significance of LSD1-expressing TNBCs. Overall, our results provide evidence that increased LSD1 protein and transcript expression in TNBCs is associated with a poorer survival rate, demonstrating that LSD1 is a promising candidate biomarker. Of note, increased protein expression was observed in patients with higher lymph node status and of Malay ethnicity. Interestingly, among Southeast Asian ethnic groups, the incidence and risk factors for TNBC

cases were reportedly more frequent in Malays [32] and correlated with shorter recurrence-free survival [33], suggesting a potential specific genetic susceptibility [34]. TNBC patients were also likelier to display lymph node metastasis at diagnosis [35], whereas patients with >10 positive LNs (N3) presented worse survival outcomes [36]. Notably, our results further demonstrated that higher *KDM1A* levels were associated with younger patients, black or African-American ethnicity, elevated Ki67 levels, and basal and BLIS molecular subtypes. At present, epidemiological data indicate that most TNBCs occur in women of African-American or black ethnicity and younger age (< 50 years old) and are associated with higher Ki67 proliferation markers [37]. In addition, patients with the BLIS subtype reportedly exhibit highly proliferative properties, dampened immune response genes and worse prognosis than other subtypes [2, 38]. Overall, the mechanism underlying *LSD1/KDM1A* overexpression seen in susceptible high-risk TNBC patients remains an area of interest for future validation as a possible early diagnostic biomarker.

With the well-established regulatory involvement of *LSD1* in extensive gene expression programs, its aberrant expression levels in association with different partner proteins are suggested in gene expression reprogramming to promote breast cancer neoplasms. Furthermore, *LSD1* transcriptional regulation is known to be cell-type specific and modulated by its associated partners [39]. As a result, our study further identified potential gene candidates associated with *LSD1* protein and transcripts.

Within the four identified DEGs between *LSD1*-positive/negative TNBCs in our study, higher expression of three genes (*COPS5*, *ELOC*, *MTDH*) was linked with poorer survival. Among the eight subunits of the CSN complex, *COPS5* functions as a critical positive regulator of cellular proliferation with a prognostic role in TNBC through negative regulation by miR-17 [40] (**Figure 9**). Surprisingly, correlation and enrichment analysis further revealed *ELOC* to be positively correlated with *COPS5* expression in all TCGA tumors [41] (**Figure 9**). The overexpression of *MTDH*, implicated in mediating breast cancer metastasis to the lungs, acts to abrogate miR-26a tumor suppressor functionality during TNBC development. [42, 43] (**Figure 9**). Moreover, while angiogenesis-related VEGF receptors are shown to be highly expressed in advanced tumor stages of 4T1 TNBC syngeneic mice [44] and our *LSD1*<sup>+</sup> patients, the lack of association with patient prognosis value suggests that *VEGFR1* may not be a reliable biomarker. Additionally, our prognostic models demonstrated that *LSD1* and three of its associated DEGs (*COPS5*, *ELOC*, *MTDH*) significantly increased prognostic power compared to classical clinicopathological parameters. These results suggest a potential clinical application of *LSD1* or its associated DEGs as independent prognostic markers, as well as when combined with IHC-based *LSD1* protein evaluation.

Among *KDM1A* high/low-expressing TNBCs across three publicly available breast cancer cohorts, overlapping differentially expressed genes were found to be involved in oncogenic regulatory pathways such as cell cycle and DNA replication. Additionally, all cell-cycle hub genes (*CDK1*, *CCNB1*, *CDC20*, *CDK2*, *CCNA2*, *CCNB2*, *CDC6*, *CHEK1*, *PLK1*, *MCM7*) had higher mRNA levels in the *KDM1A*<sup>high</sup> TNBC subgroup. Notably, higher expression of two hub genes (*CDC6* and *PLK1*) was associated with significantly worse survival rates. The initiation of DNA replication is tightly regulated by the stepwise assembly of the Prereplication complex (Pre-RC) during the G1 phase, which consists of the origin-recognition complex (ORC), Cdt1, Cdc6 and the MCM complex [45]. Mechanistically, *LSD1* levels peak in the early S phase to facilitate origin firing (via TICRR loading and subsequent *CDC45* recruitment) in H3K4me2-enriched euchromatin regions as preferred sites of pre-RC binding [46]. Evidence has shown that higher levels of Cdc6 are associated with poorer

survival in breast cancer patients [47], whereby concomitant aberrancy in LSD1-mediated epigenetic regulation in the activation of replication origin may be linked with abnormal DNA replication processes (**Figure 10**). Similarly, PLK1 is overexpressed in TNBC patients as a key regulator of increased mitosis through the G2-M phase [48]. In TNBC, the overexpression of Plk1 (in cooperation with amplified SCYL1 and TEX14) phosphorylates the tumor suppressor REST at Ser1030, leading to the degradation of REST to cause tumor growth and metastatic expansion [49]. Nevertheless, LSD1 can directly regulate Plk1 expression by binding to its promoter region to induce tumor cell proliferation and migration [50] (**Figure 10**).

Moving beyond, other therapeutic strategies are also being explored to enhance the immune system for the elimination of cancer cells. As alluded to earlier, *KDM1A* levels were interestingly enriched in the BLIS molecular subtype, previously characterized by aggressive proliferation, downregulation of immune-regulating pathways (B cell, T cell, and natural killer cell) and cytokine pathways. Importantly, many studies have demonstrated that LSD1 ablation enhances tumor immunogenicity in poorly immunogenic cancers [15-17]. In line with previous findings, we found LSD1 prognostic DEGs (*COPS5*, *ELOC*) and LSD1 mRNA expression to be negatively correlated with immune signature genes such as CD3, CD4 and CD8 across different TNBC cohorts. Overall, our results further support the notion that abnormal epigenetic modifications of LSD1 govern the silencing of breast tumor immunity, whereby LSD1 inhibition may be a novel therapeutic strategy for poorly immunogenic breast cancers.

Previous associated studies on the biological function and expression patterns of our prognostic gene signatures suggest that LSD1/*KDM1A*-expressing TNBCs facilitate the activation of aberrant cell cycle regulation. Nevertheless, our study has several limitations. First, FPPE blocks used in TMA construction were dated back from 2003 to 2014, and the tissue quality may contribute to reduced antigenicity and sensitivity for IHC reaction, leading to decreased protein detection. Next, publicly available expression data were only analyzed through a series of computational methods without *in vitro/in vivo* validation of the detailed regulatory mechanism within TNBC heterogeneity. Thus, future research is required to address the clinical relevance and functionality of the identified prognostic gene candidates in larger LSD1+ TNBC studies using wet assays.

In conclusion, our study correlates LSD1+ expression with poorer survival in a subgroup of Asian TNBC patients. Since epigenetic modifiers and their associated partners are increasingly being studied in regulating broad gene expression programs that contribute to breast neoplasms, the identification of prognostic genes associated with LSD1 biological functions could have remarkable diagnostic and prognostic value in LSD1+ TNBCs and, by extension, in LSD1+ pancancers.

## **FIGURES**

**Figure 1.** LSD1 expression and association with survival outcomes in TNBC patients

- A) Tissue microarray sections with immunohistochemical LSD1 nuclear staining in TNBC.
- B) Kaplan-Meier analysis of disease-free survival (DFS) outcomes in LSD1-expressing TNBCs.
- C) Kaplan-Meier analysis of overall survival (OS) outcomes in LSD1-expressing TNBCs.

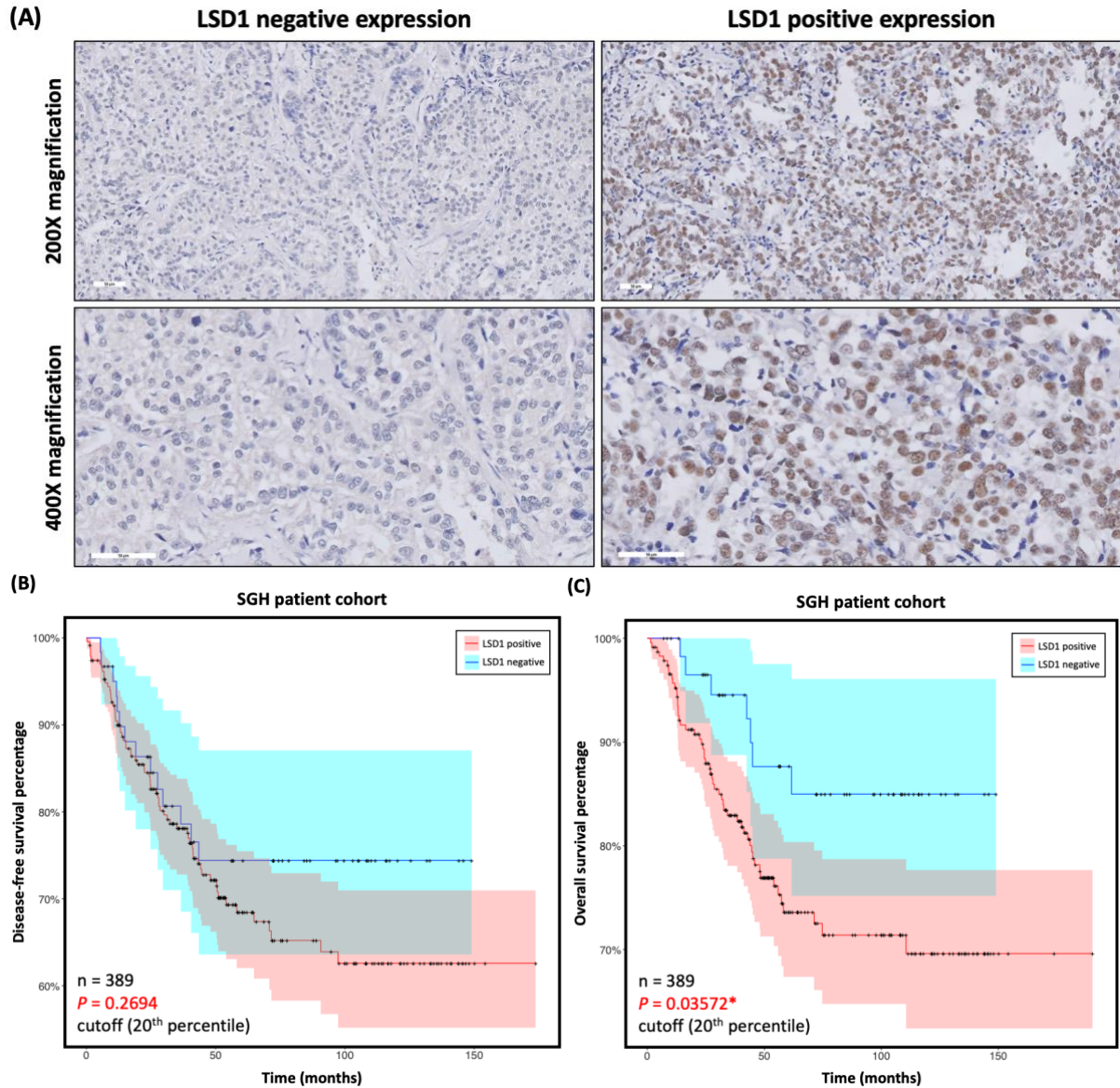
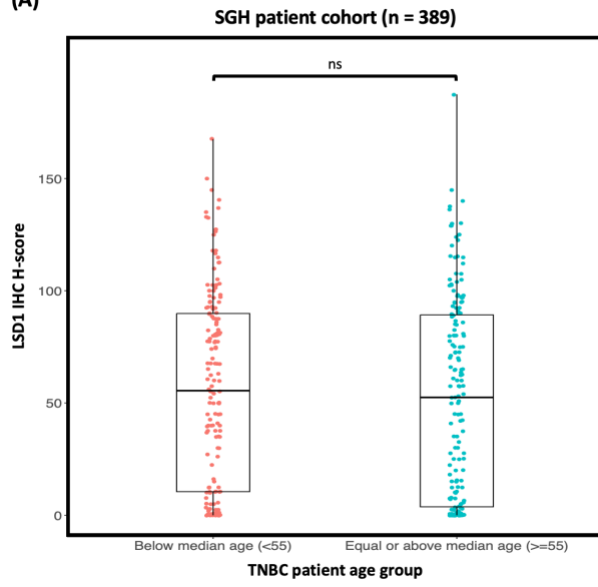


**Figure 2.** LSD1 expression level in different clinicopathological features in the SGH cohort  
 A) Violin chart of LSD1 expression levels in different patient age groups.  
 B) Violin chart of LSD1 expression levels in different histological grades.  
 C) Violin chart of LSD1 expression levels in different lymph node statuses.  
 D) Violin chart of LSD1 expression levels in different patient races.  
 E) Violin chart of LSD1 expression levels in different tumor sizes.

(A)



(B)

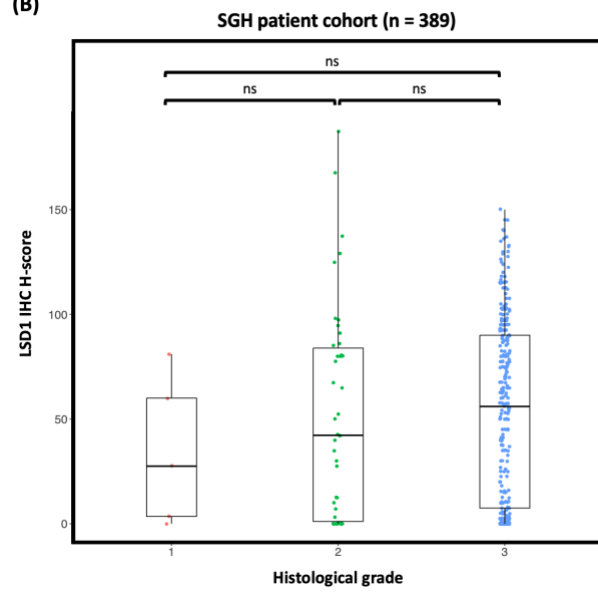




**Figure 3.** Differentially expressed genes between the “LSD1 positive” and “LSD1 negative” groups in the SGH TNBC cohort

A) Volcano plot of the identification of significant differentially-expressed genes among the SGH NanoString gene panel.

B) Violin chart of *COPS5* mRNA expression levels between the LSD1-positive/negative groups.

C) Violin chart of *ELOC* mRNA expression levels between the LSD1-positive/negative groups.

D) Violin chart of *MTDH* mRNA expression levels between the LSD1-positive/negative groups.

E) Violin chart of *VEGFR1* mRNA expression levels between the LSD1-positive/negative groups.

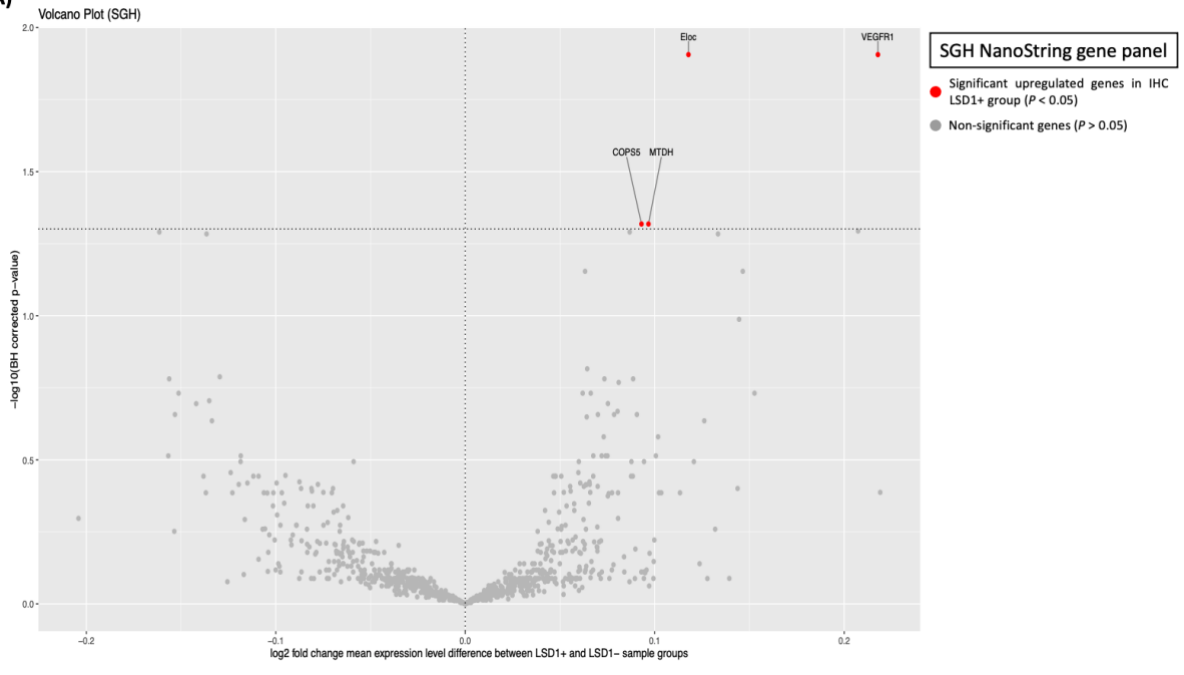
F) Survival analysis of *COPS5* mRNA expression in the SGH TNBC cohort.

G) Survival analysis of *ELOC* mRNA expression in the SGH TNBC cohort.

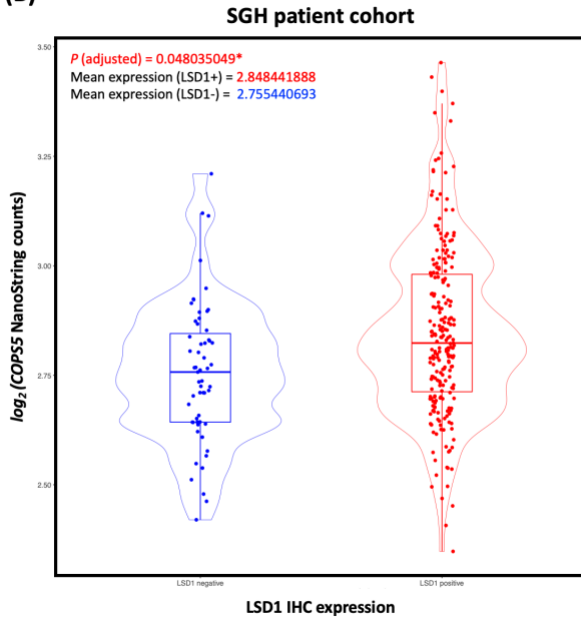
H) Survival analysis of *MTDH* mRNA expression in the SGH TNBC cohort.

I) Survival analysis of *VEGFR1* mRNA expression in the SGH TNBC cohort.

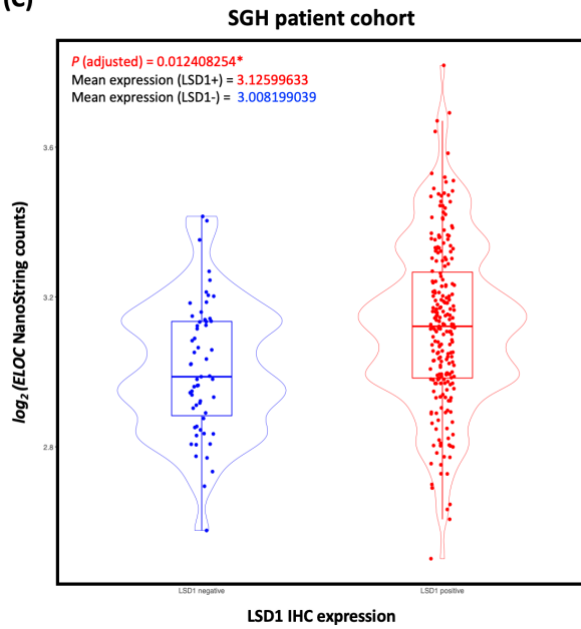
(A)



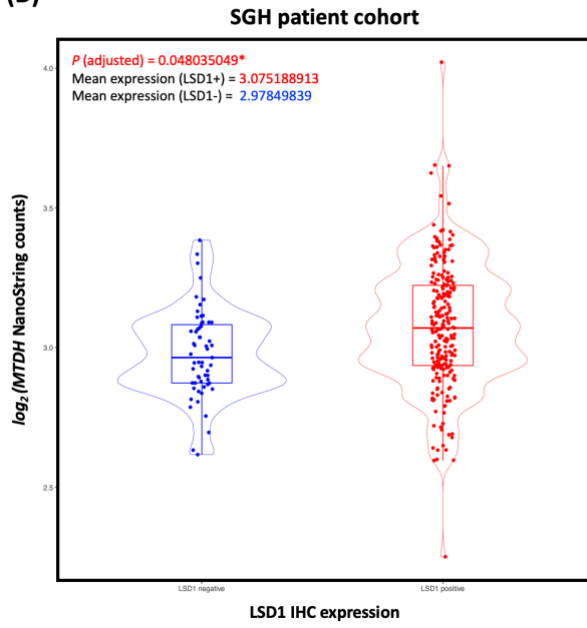
(B)



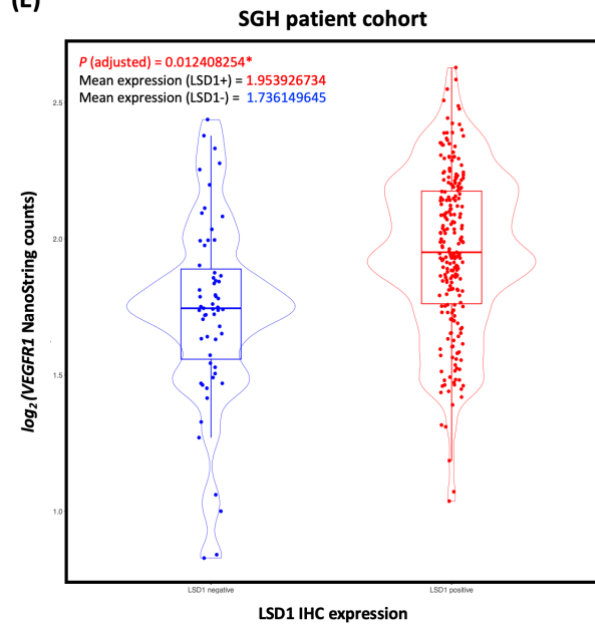
(C)



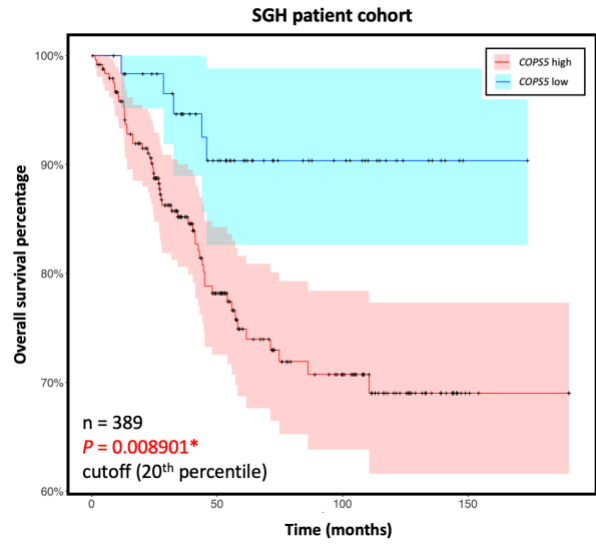
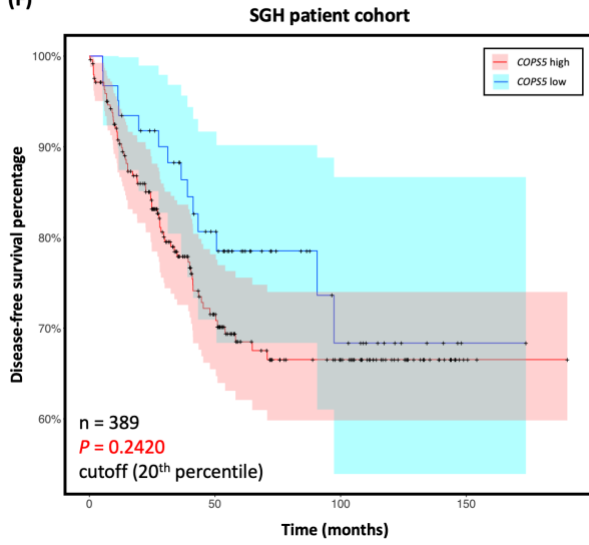
(D)



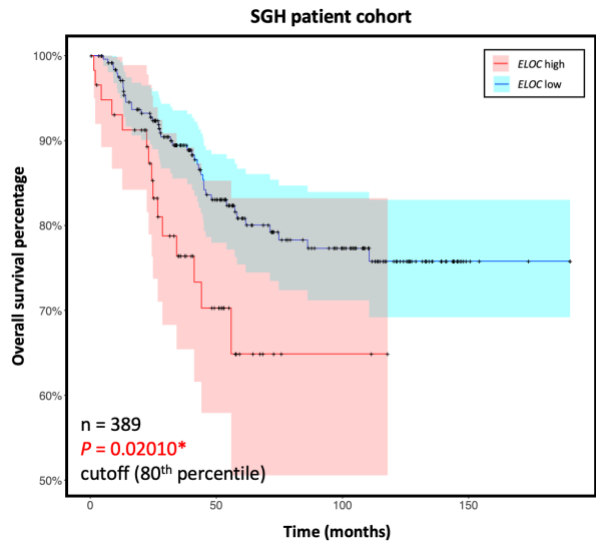
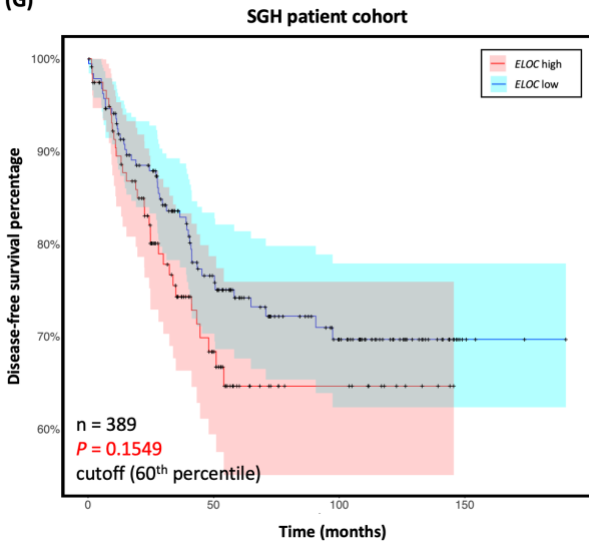
(E)



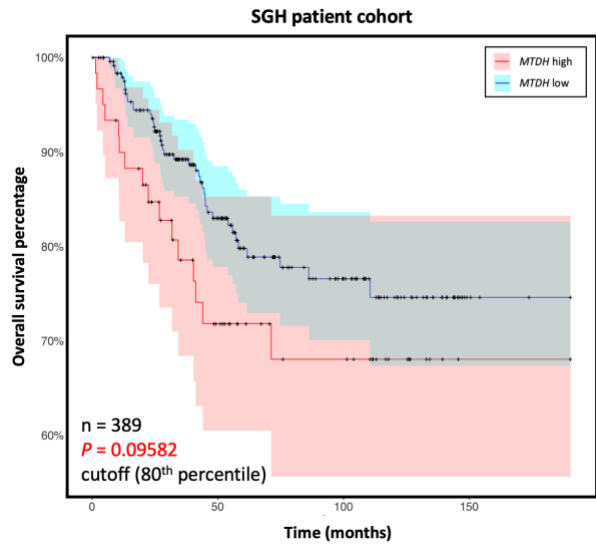
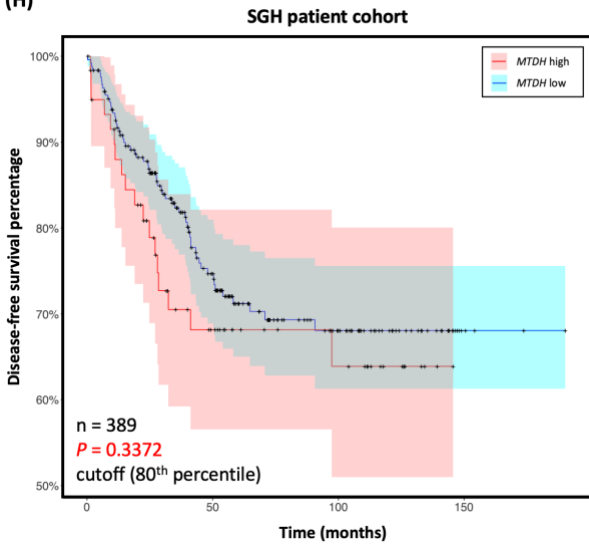
(F)



(G)



(H)



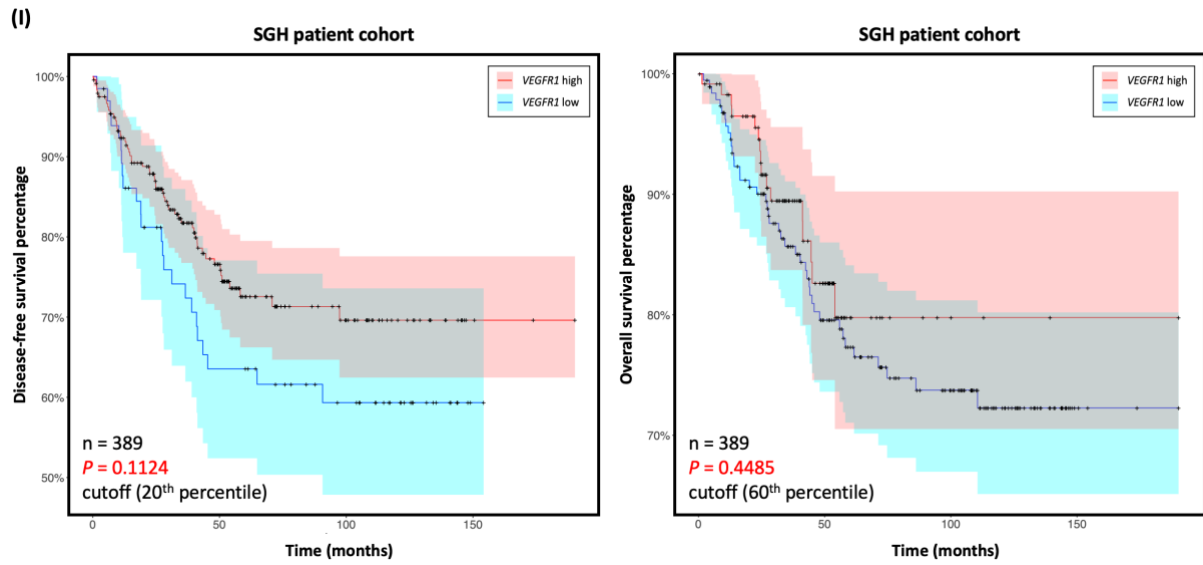


**Figure 4.** Expression level of a panel of four significant DEGs in LSD1-expressing TNBC patients

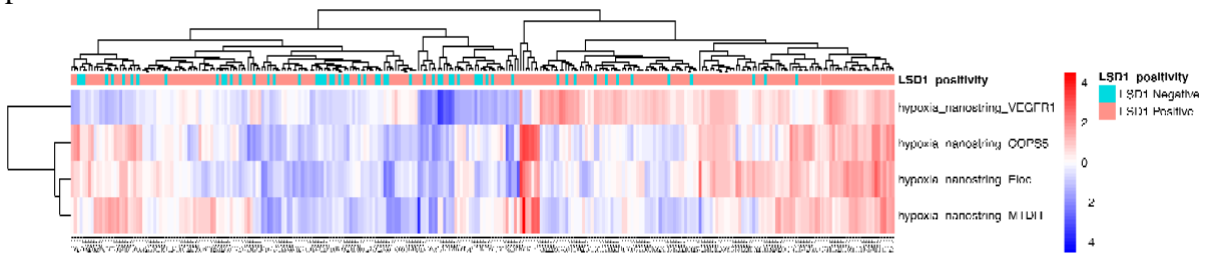
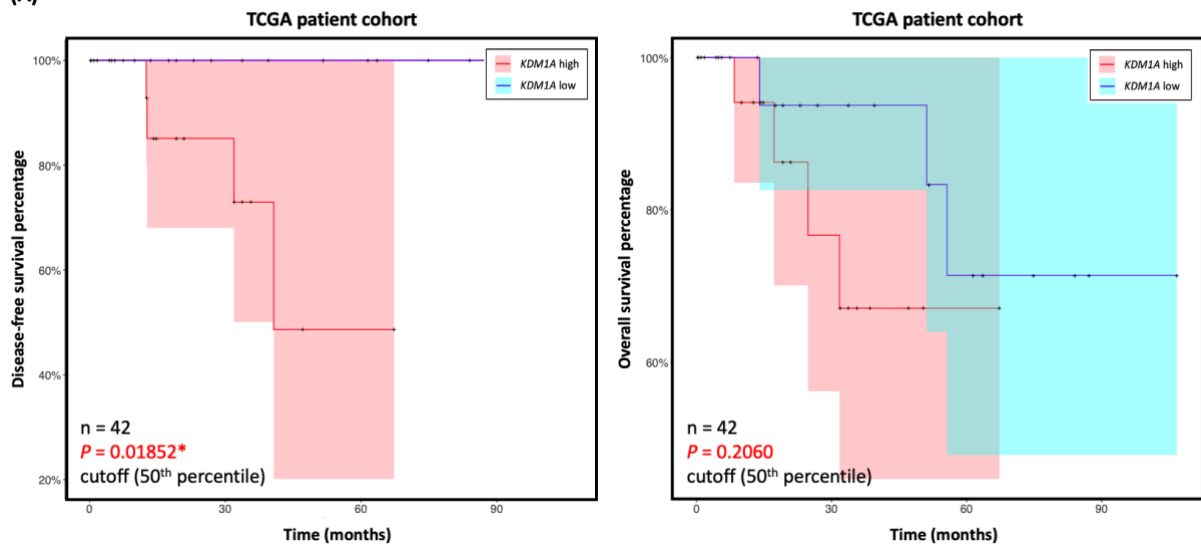


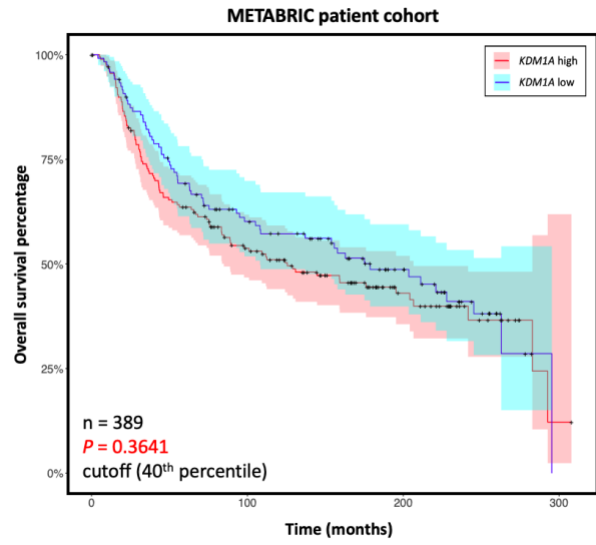
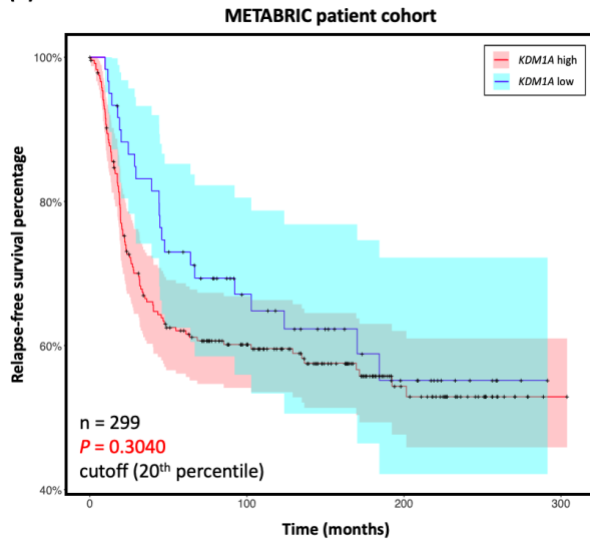
**Figure 5.** KDM1A gene expression and association with TNBC survival outcomes in three public breast cancer cohorts

- A) KDM1A expression in the TCGA TNBC cohort.
- B) KDM1A expression in the METABRIC TNBC cohort.
- C) KDM1A expression in the FUSCC TNBC cohort.

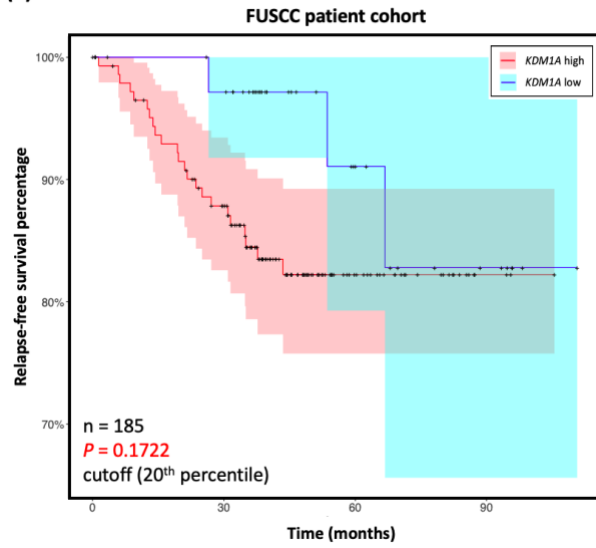
(A)



(B)

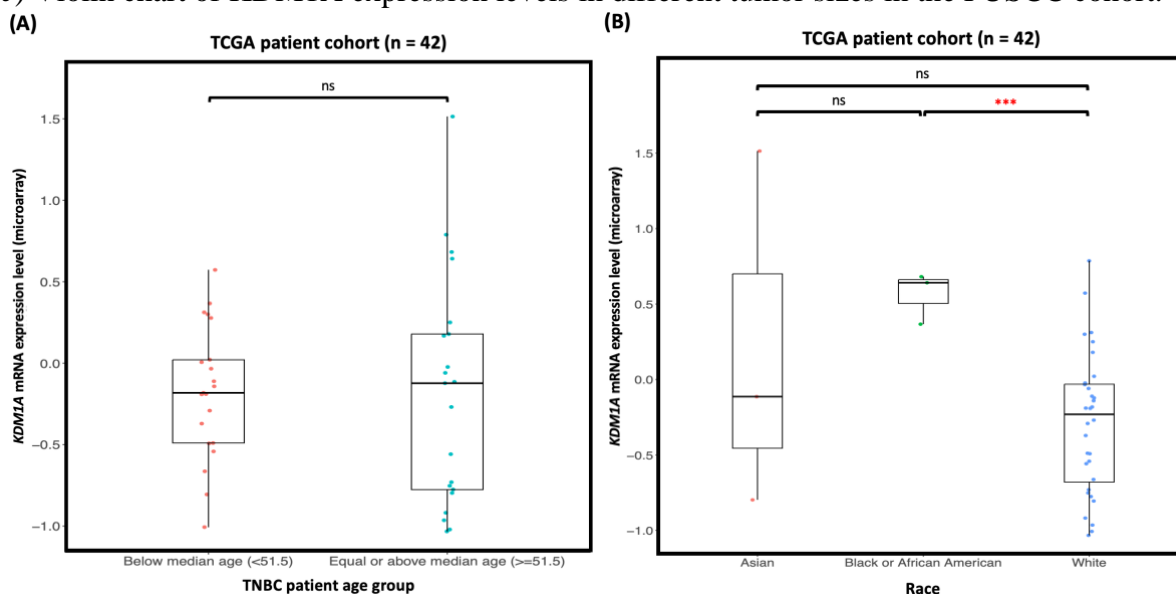


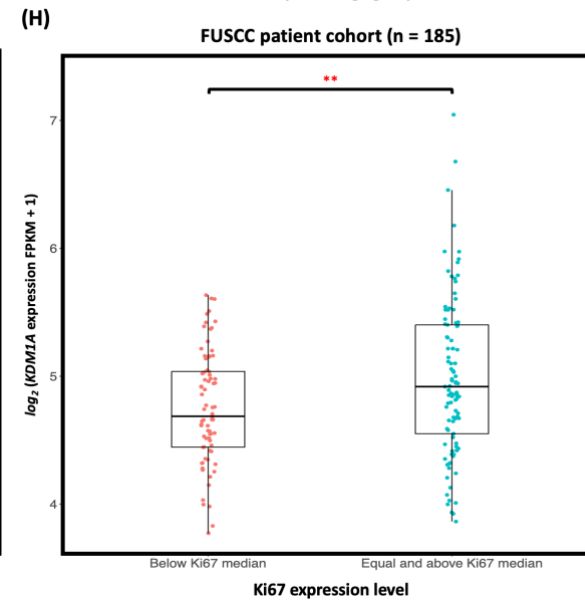
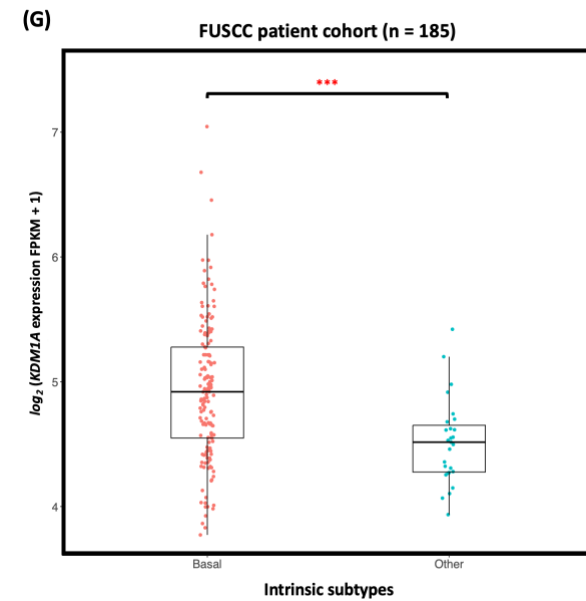
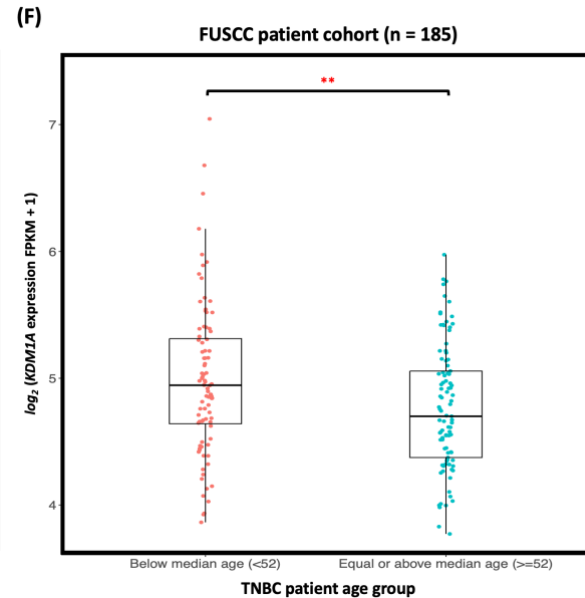
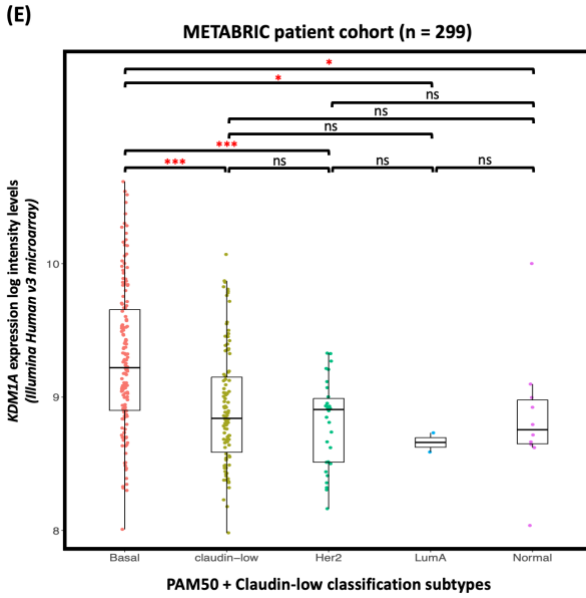
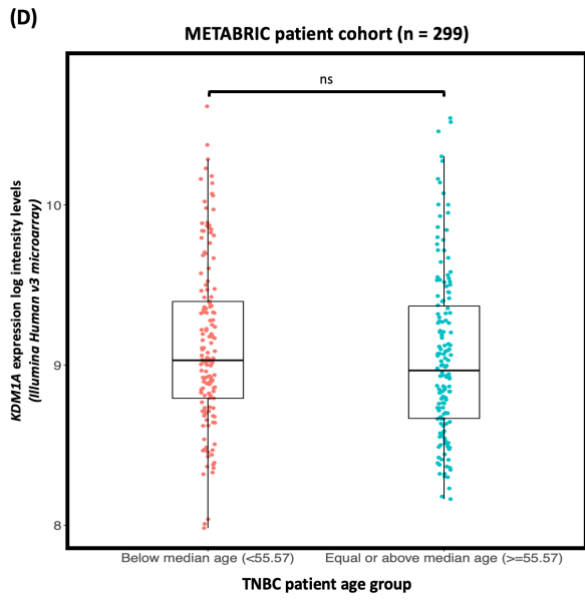
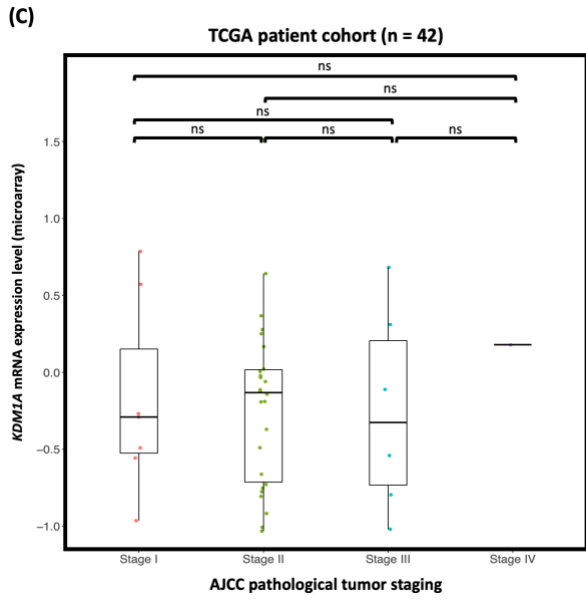
(C)



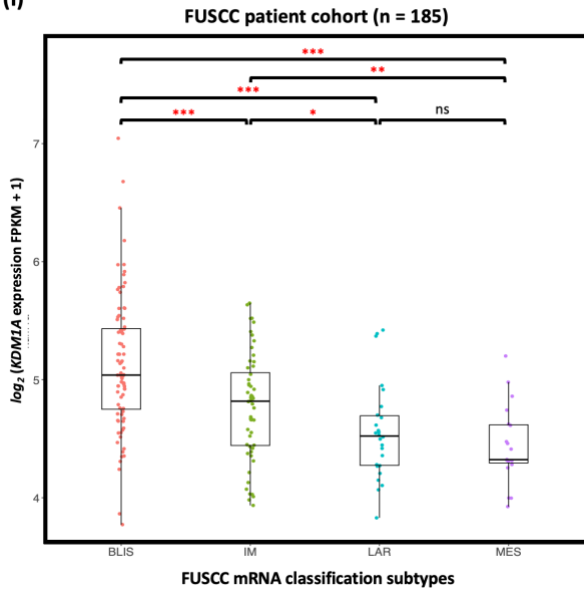
**Figure 6.** KDM1A gene expression levels in different clinicopathological features in three public breast cancer cohorts

- A) Violin chart of KDM1A expression levels in different patient age groups in the TCGA cohort.
- B) Violin chart of KDM1A expression levels in different patient races in the TCGA cohort.
- C) Violin chart of KDM1A expression levels in different AJCC pathologic stages in the TCGA cohort.
- D) Violin chart of KDM1A expression levels in different patient age groups in the METABRIC cohort.
- E) Violin chart of KDM1A expression levels in different PAM50 + claudin-low classifications in the METABRIC cohort.
- F) Violin chart of KDM1A expression levels in different patient age groups in the FUSCC cohort.
- G) Violin chart of KDM1A expression levels in different intrinsic subtypes in the FUSCC cohort.
- H) Violin chart of KDM1A expression levels at different Ki67 levels in the FUSCC cohort.
- I) Violin chart of KDM1A expression levels in different FUSCC mRNA classifications in the FUSCC cohort.
- J) Violin chart of KDM1A expression levels in different tumor sizes in the FUSCC cohort.





(I)



(J)

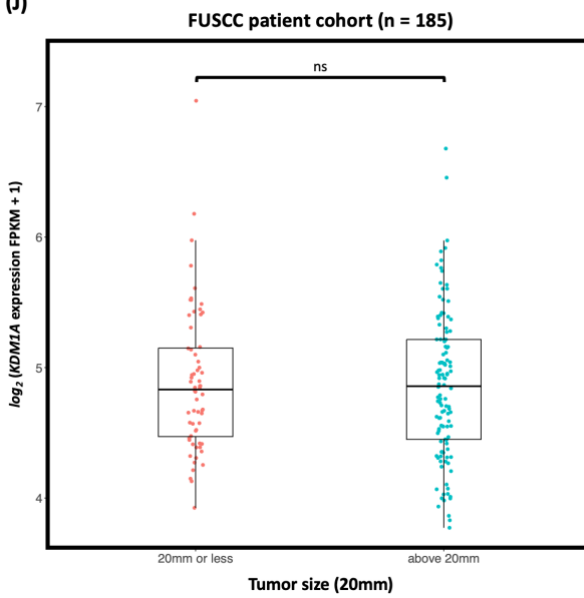
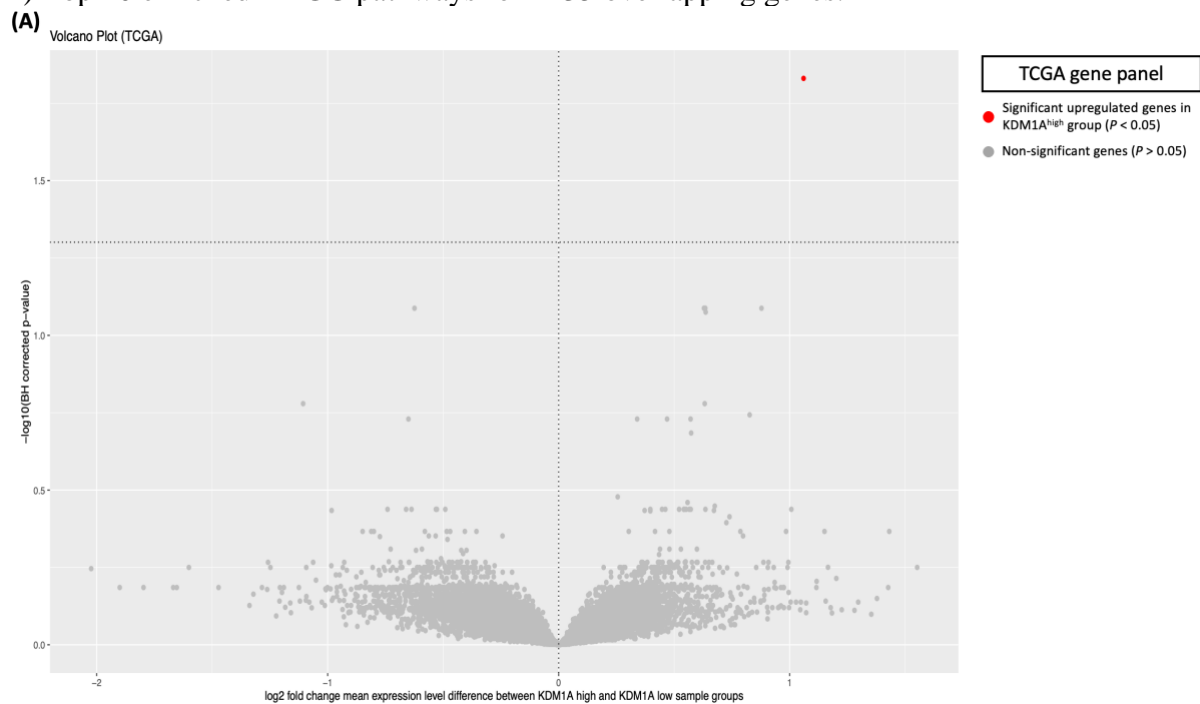
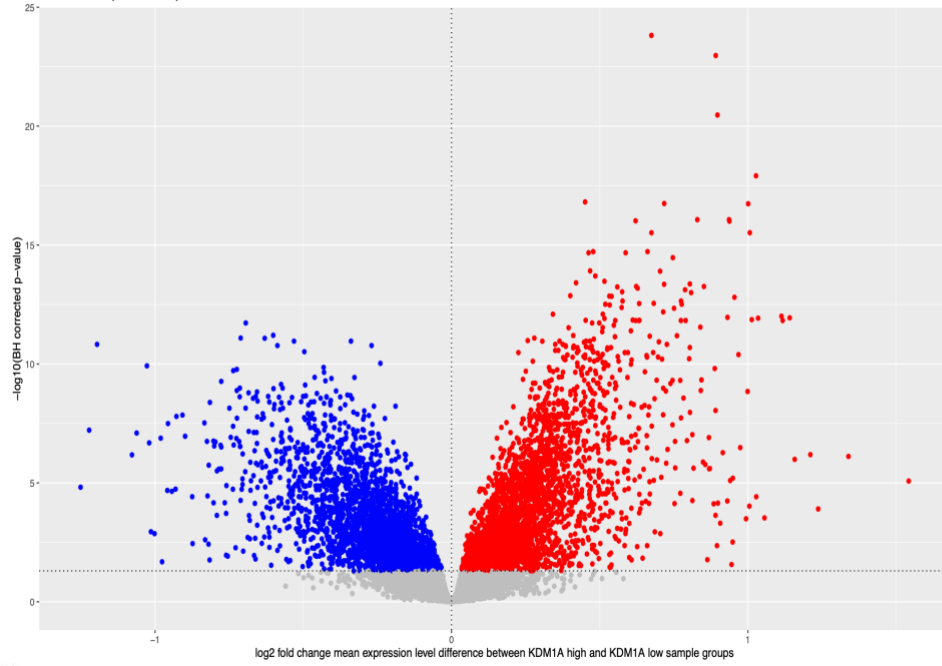


**Figure 7.** Differentially expressed genes between the “KDM1A high” and “KDM1A low” groups in three public breast cancer cohorts

- A) Volcano plot of significantly differentially expressed genes among the TCGA gene panel.
- B) Volcano plot of significantly differentially expressed genes among the METABRIC gene panel.
- C) Volcano plot of significantly differentially expressed genes among the FUSCC gene panel.
- D) Venn diagram of overlapping significant DEGs in all three cohorts.
- E) Top 20 enriched KEGG pathways for 2135 overlapping genes.



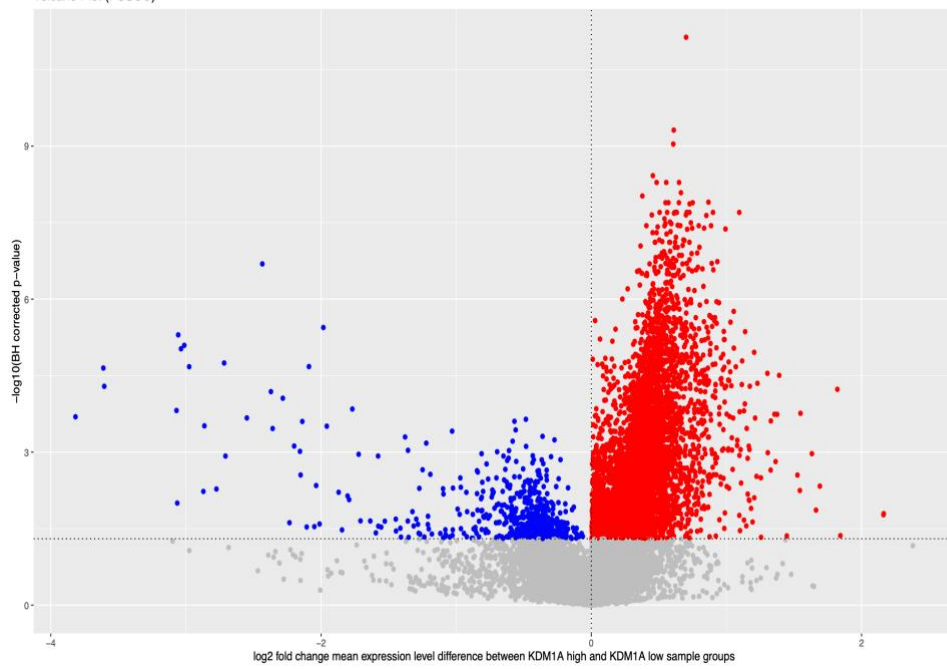
(B) Volcano Plot (METABRIC)



**METABRIC gene panel**

- Significant upregulated genes in KDM1A<sup>hi</sup> group ( $P < 0.05$ )
- Significant downregulated genes in KDM1A<sup>hi</sup> group ( $P < 0.05$ )
- Non-significant genes ( $P > 0.05$ )

(C) Volcano Plot (FUSCC)



**FUSCC gene panel**

- Significant upregulated genes in KDM1A<sup>hi</sup> group ( $P < 0.05$ )
- Significant downregulated genes in KDM1A<sup>hi</sup> group ( $P < 0.05$ )
- Non-significant genes ( $P > 0.05$ )

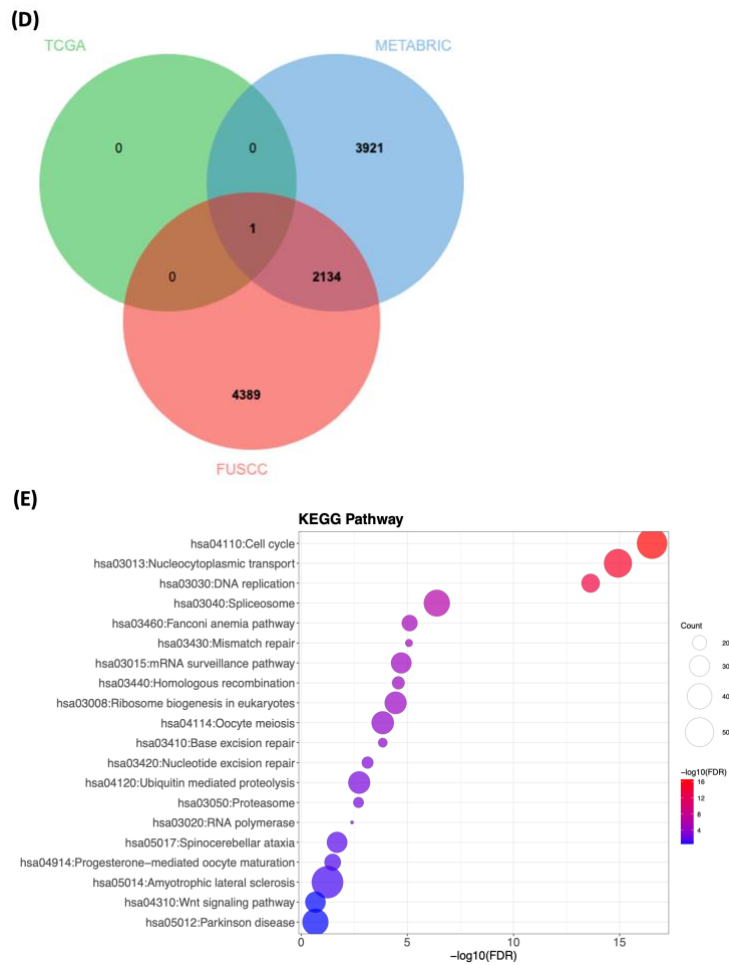


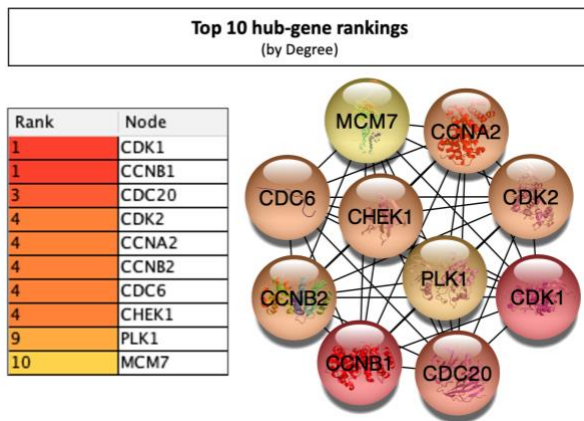
**Figure 8.** Identification of cell cycle-associated hub genes in KDM1A-expressing TNBCs  
 A) PPI network construction of cell cycle-related genes.  
 B) PPI network construction of the top 10 cell cycle-associated hub genes.  
 C) Violin chart of *CDK1* mRNA expression levels between the KDM1A high/low groups.  
 D) Violin chart of *CCNB1* mRNA expression levels between the KDM1A high/low groups.  
 E) Violin chart of *CDC20* mRNA expression levels between the KDM1A high/low groups.

- F) Violin chart of *CDK2* mRNA expression levels between the KDM1A high/low groups.
- G) Violin chart of *CCNA2* mRNA expression levels between the KDM1A high/low groups.
- H) Violin chart of *CCNB2* mRNA expression levels between the KDM1A high/low groups.
- I) Violin chart of *CDC6* mRNA expression levels between the KDM1A high/low groups.
- J) Violin chart of *CHEK1* mRNA expression levels between the KDM1A high/low groups.
- K) Violin chart of *PLK1* mRNA expression levels between the KDM1A high/low groups.
- L) Violin chart of *MCM7* mRNA expression levels between the KDM1A high/low groups.

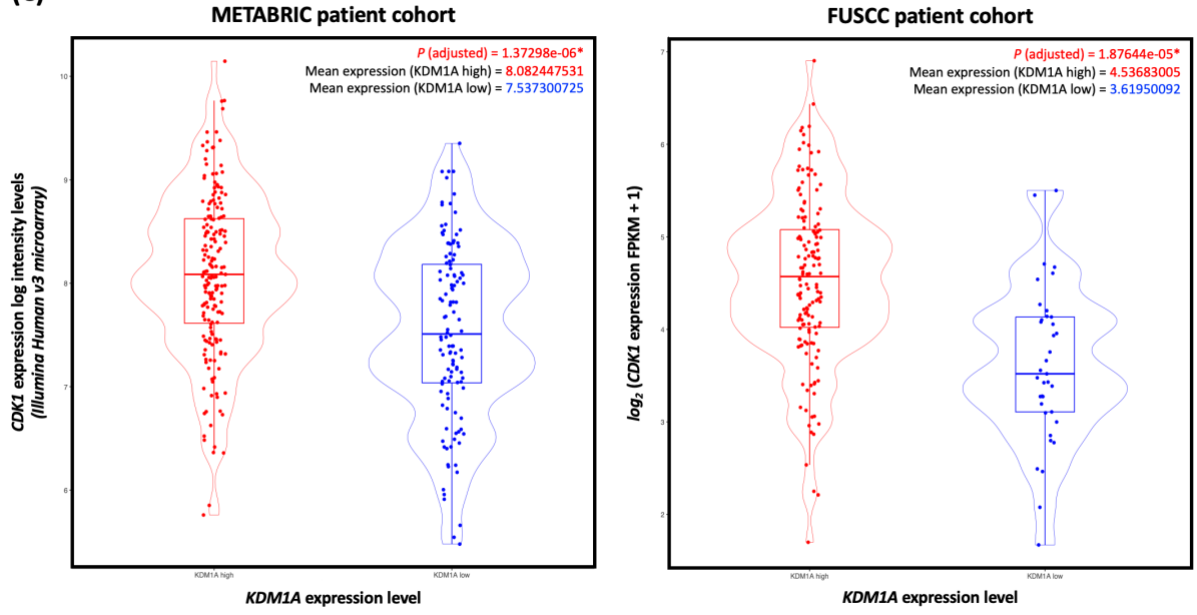
(A)



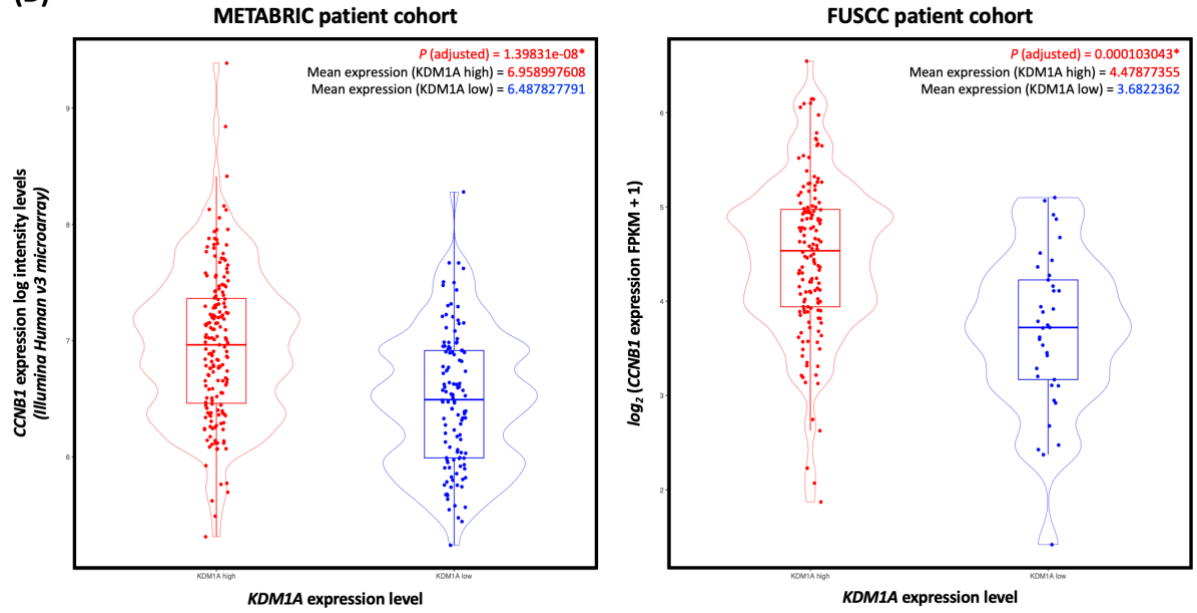
(B)



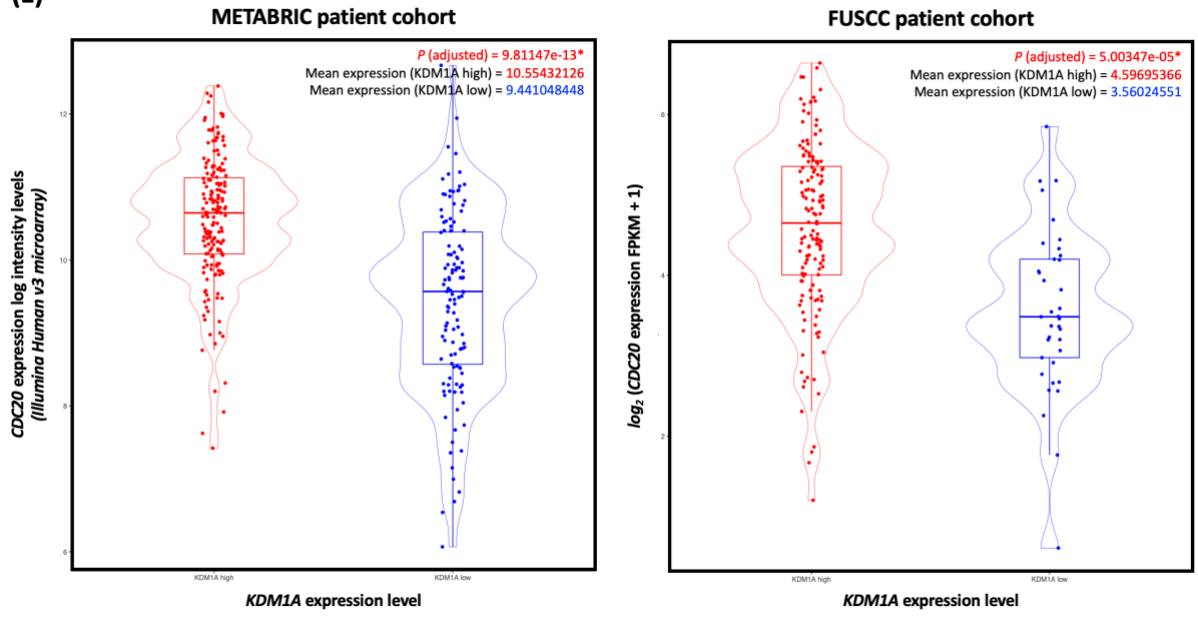
(C)



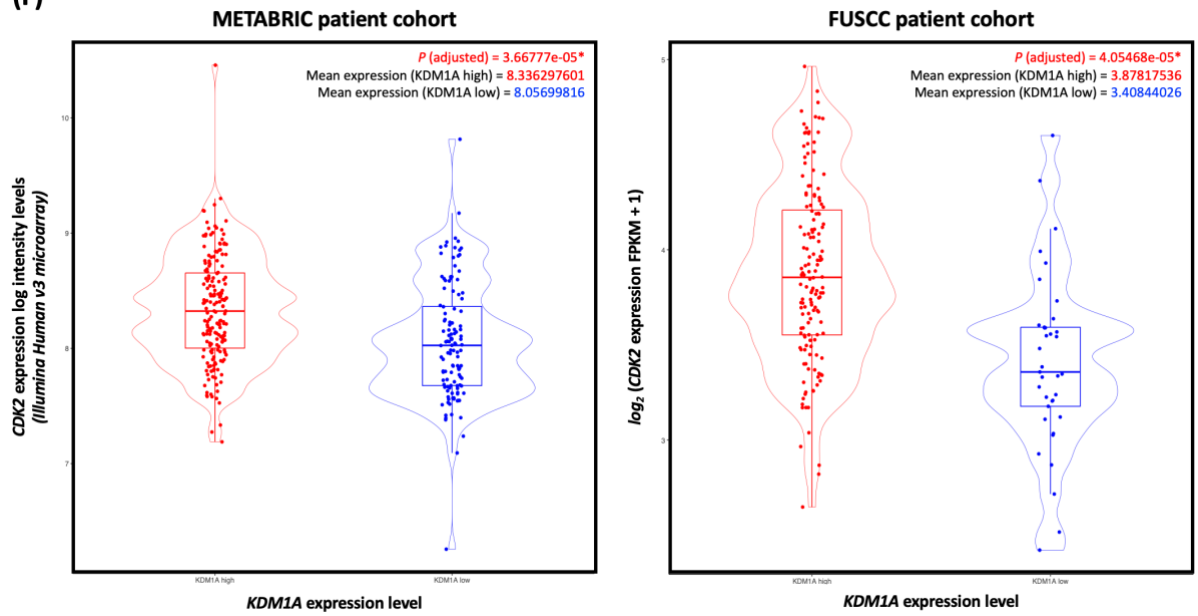
(D)



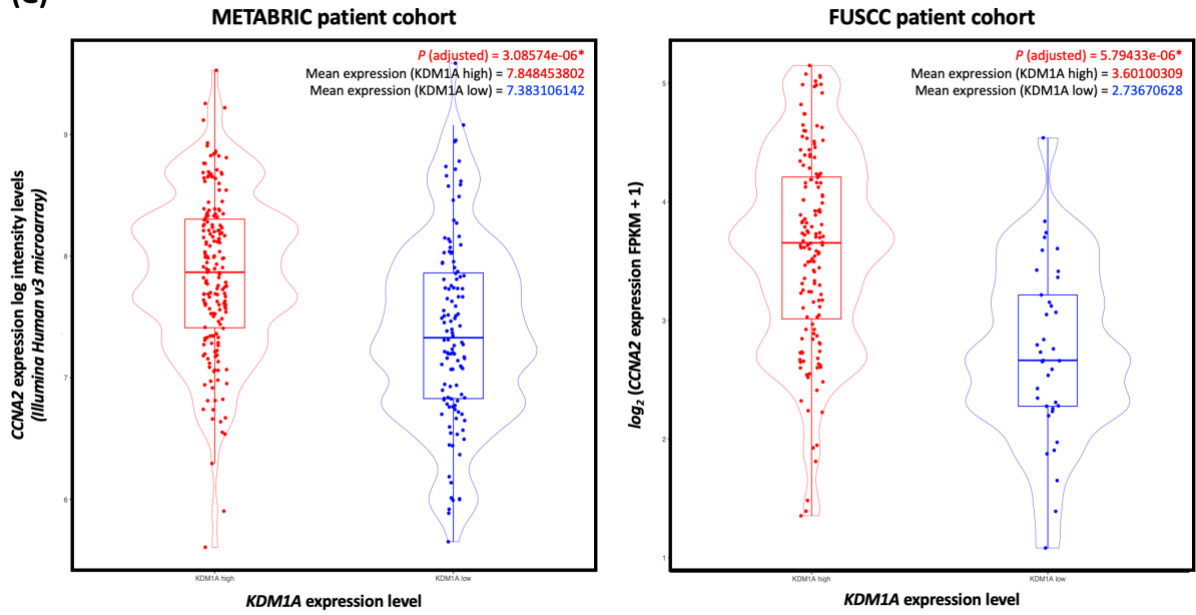
(E)



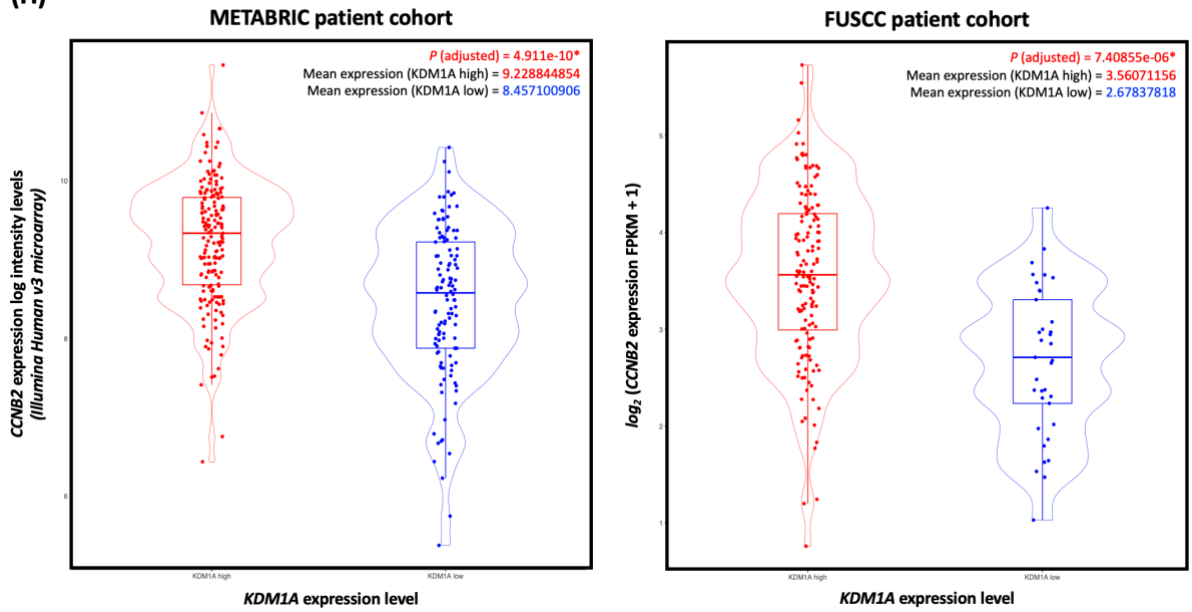
(F)



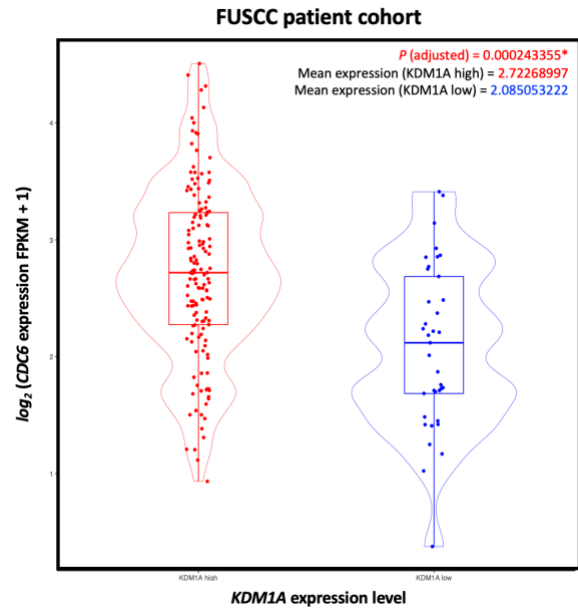
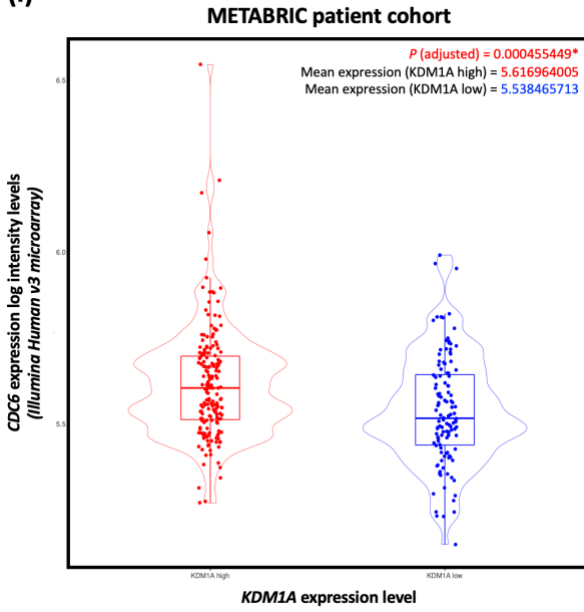
(G)



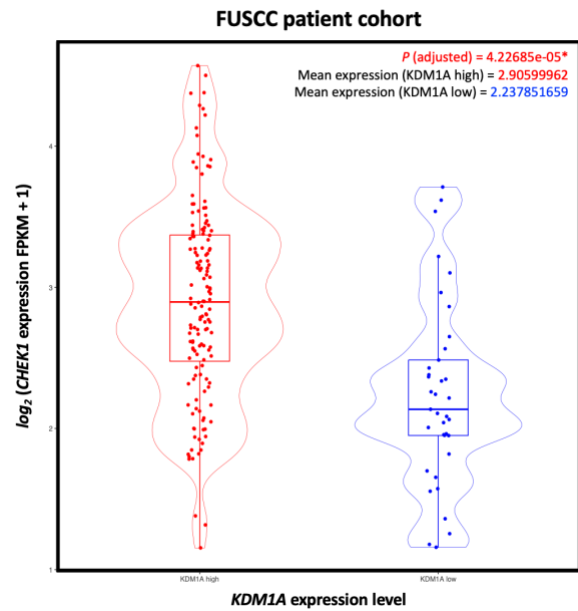
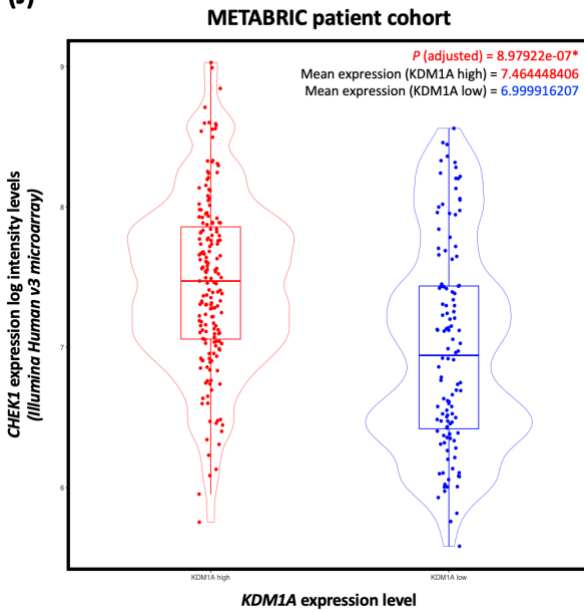
(H)



(I)



(J)



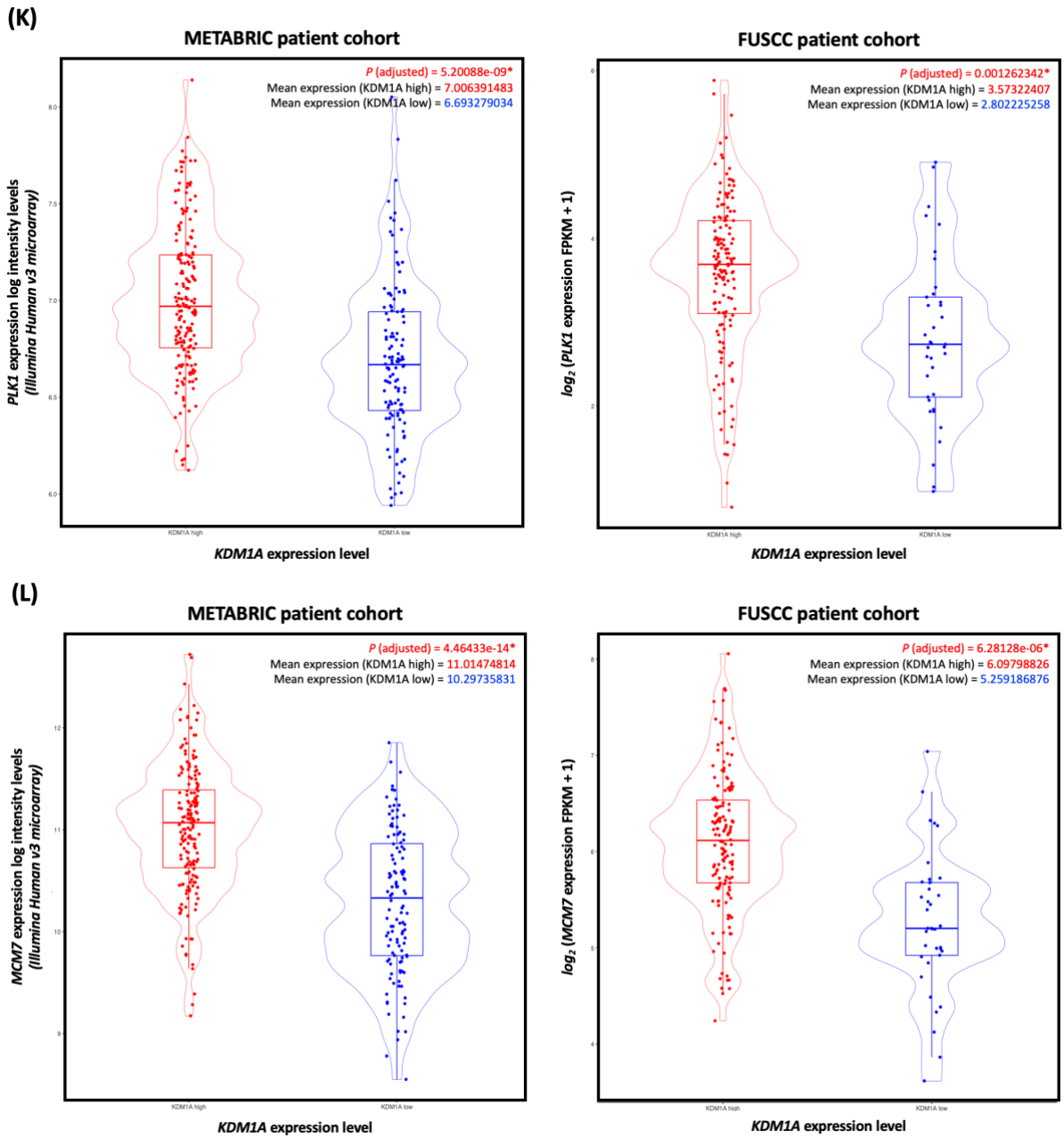


**Figure 9.** Proposed schematic diagram of the LSD1-mediated oncogenic shift in TNBCs via transcriptional regulation of prognostic LSD1-associated genes. Figure created with BioRender.com

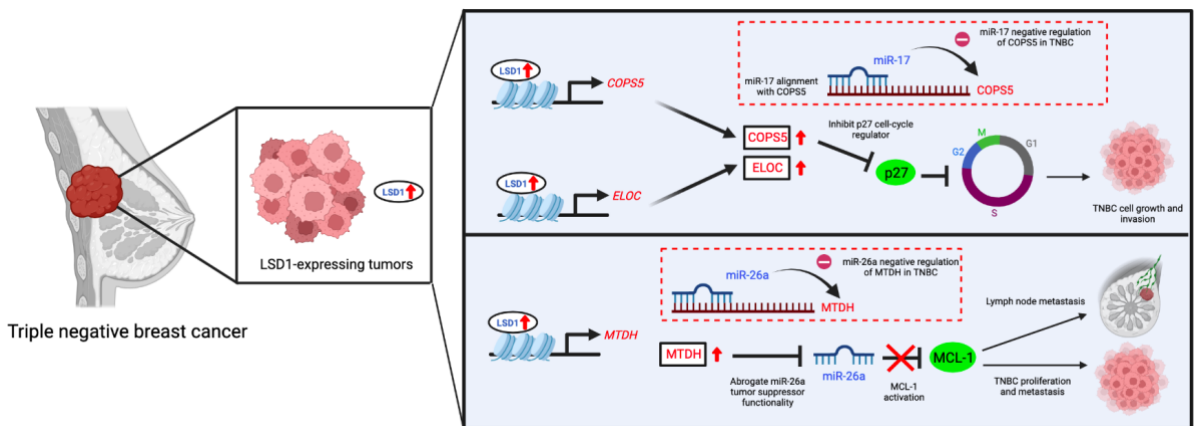


**Figure 10.** Proposed schematic diagram of the KDM1A-mediated oncogenic shift in TNBCs via transcriptional regulation of prognostic cell cycle hub genes. Figure created with BioRender.com

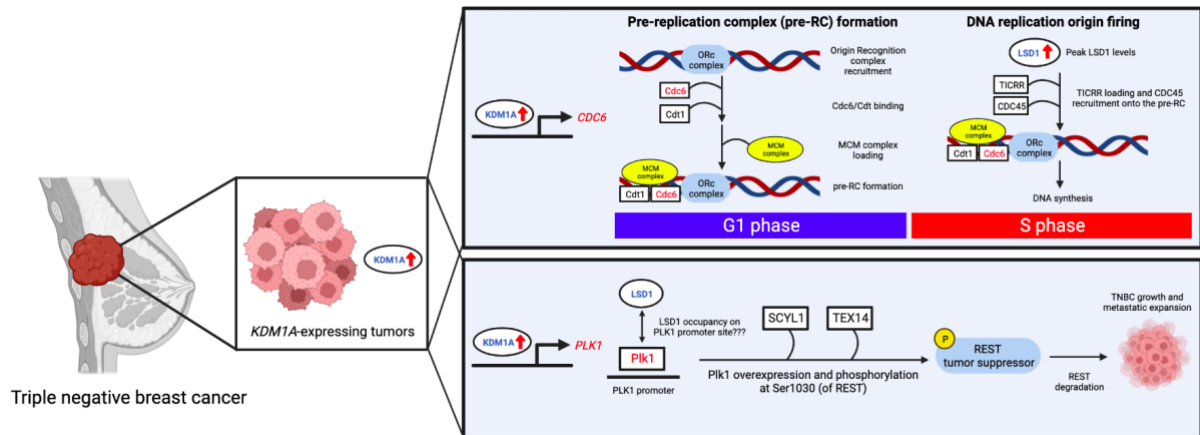


**Figure 11.** Spearman correlation plot between LSD1/*KDM1A* and key immune-response genes

- A) LSD1/*LSD1*-associated DEGs and immune-response genes in the SGH cohort.
- B) *KDM1A*/*KDM1A*-associated cell cycle hub genes and immune-response genes in the METABRIC cohort.
- C) *KDM1A*/*KDM1A*-associated cell cycle hub genes and immune-response genes in the FUSCC cohort.
- D) *KDM1A*/*KDM1A*-associated cell cycle hub genes and immune-response genes in the TCGA cohort.

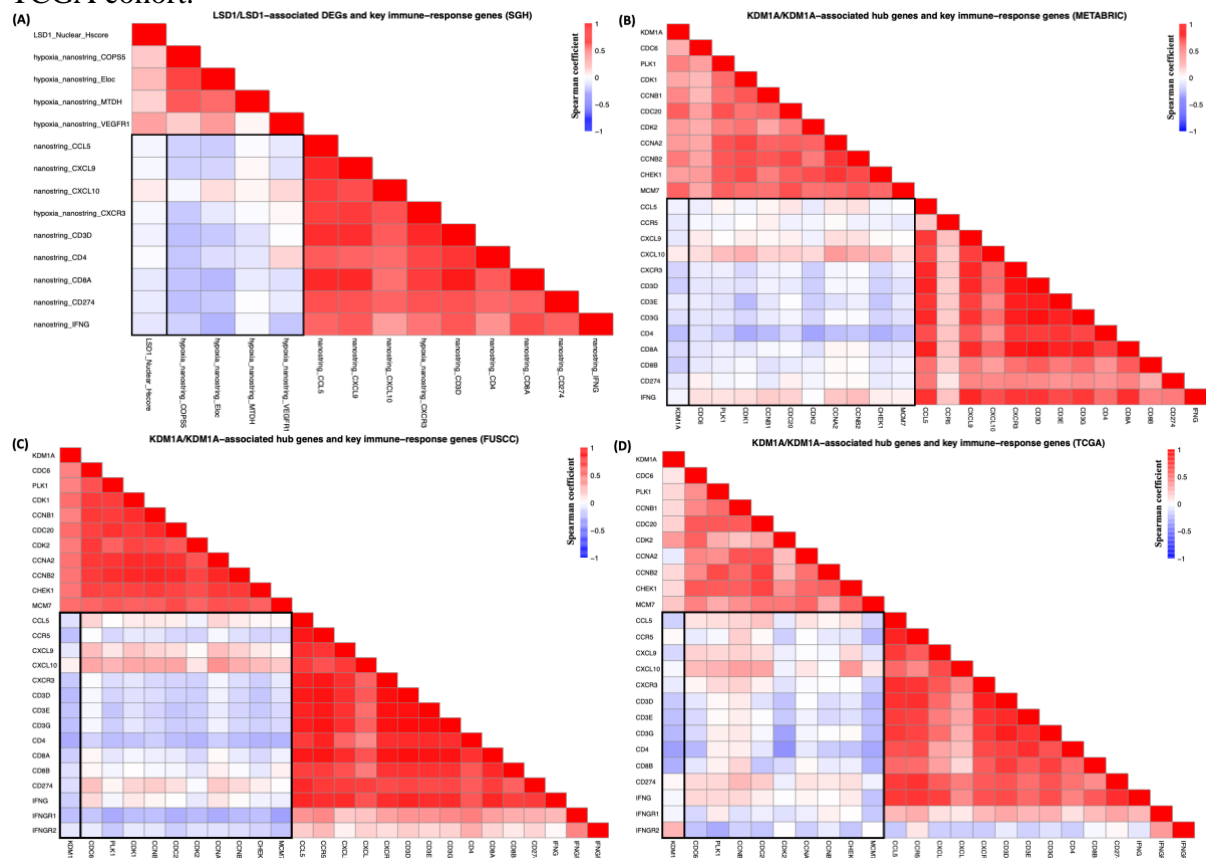


**Table 1.** Log-likelihood change of models with added individual prognostic terms

Survival predictor variables	DFS				OS			
	$\Delta LR_{\chi^2}$	AIC	Logrank p-value	Logrank test	$\Delta LR_{\chi^2}$	AIC	Logrank p-value	Logrank test
CP	Reference	769.064716	1.27e-06	32.8641354	Reference	536.602275	1.15e-09	47.5918377
CP + LSD1 vs. CP	0.31367514	703.948688	7.88e-06	31.378972	1.79726237	504.430777	1.56e-09	49.7458907
CP + <i>COPSS</i> vs. CP	0.14319614	662.110661	9.78e-06	30.9054851	0.37817523	463.060931	5.24e-09	47.1737134
CP + <i>ELOC</i> vs. CP	0.00972638	662.3776	1.10e-05	30.6385456	0.60963861	462.598005	4.21e-09	47.6366402
CP + <i>MTDH</i> vs. CP	0.74980217	660.897449	5.63e-06	32.1186971	0.17470811	463.467866	6.34e-09	46.7667792
CP + <i>VEGFR1</i> vs. CP	0.2747658	661.847521	8.68e-06	31.1686244	0.02014521	463.776991	7.33e-09	46.4576534

**Table 2.** Log-likelihood change in the LSD1 model with added gene prognostic terms

Survival predictor variables	DFS				OS			
	$\Delta LR_{\chi^2}$	AIC	Logrank p-value	Logrank test	$\Delta LR_{\chi^2}$	AIC	Logrank p-value	Logrank test
CP <sup>LSD1</sup>	Reference	703.948688	7.88e-06	31.378972	Reference	504.430777	1.56e-09	49.7458907
CP <sup>LSD1</sup> + <i>COPSS</i> vs. CP <sup>LSD1</sup>	0.05827449	601.064515	3.98e-05	29.9739515	0.33826033	435.170522	1.24e-08	47.8951807
CP <sup>LSD1</sup> + <i>ELOC</i> vs. CP <sup>LSD1</sup>	0.00870851	601.163647	4.15e-05	29.8748196	0.35136828	435.144306	1.23e-08	47.9213966
CP <sup>LSD1</sup> + <i>MTDH</i> vs. CP <sup>LSD1</sup>	0.78642045	599.608223	2.10e-05	31.4302434	0.08757797	435.671886	1.56e-08	47.393816
CP <sup>LSD1</sup> + <i>VEGFR1</i> vs. CP <sup>LSD1</sup>	0.443071	600.294922	2.84e-05	30.7435445	0.00073952	435.845563	1.69e-08	47.2201391

**Table 3.** Summary of comparative survival analysis for cell cycle-associated hub genes

Patient cohort	Cell-cycle linked hub genes	Expression level	Relapse free survival (P value)	Overall survival (P value)
FUSCC	<i>CDK1</i>	High	<i>Better</i> (P = 0.1)	Not available
METABRIC		High	Poor (P = 0.4)	<i>Better</i> (P = 0.2)
FUSCC	<i>CCNB1</i>	High	Poor (P = 0.4)	Not available
METABRIC		High	Poor (P = 0.2)	Poor (P = 0.3)
FUSCC	<i>CDC20</i>	High	Poor (P = 0.3)	Not available
METABRIC		High	Poor (P = 0.08)	Poor (P = 0.2)
FUSCC	<i>CDK2</i>	High	<i>Better</i> (P = 0.4)	Not available
METABRIC		High	Poor (P = 0.3)	<i>Better</i> (P = 0.2)
FUSCC	<i>CCNA2</i>	High	Poor (P = 0.1)	Not available
METABRIC		High	<i>Better</i> (P = 0.3)	<i>Better</i> (P = 0.1)
FUSCC	<i>CCNB2</i>	High	Poor (P = 0.5)	Not available
METABRIC		High	Poor (P = 0.3)	<i>Better</i> (P = 0.1)
FUSCC	<i>CDC6</i>	High	<i>Better</i> (P = 0.1)	Not available
METABRIC		High	<b>Poor</b> (P = 0.01*)	<b>Poor</b> (P = 0.02*)
FUSCC	<i>CHEK1</i>	High	<i>Better</i> (P = 0.08)	Not available

METABRIC		High	Poor (P = 0.2)	Poor (P = 0.4)
FUSCC	<i>PLK1</i>	High	Poor (P = 0.1)	Not available
METABRIC		High	<b>Poor</b> (P = 0.05*)	Poor (P = 0.06)
FUSCC	<i>MCM7</i>	High	<i>Better</i> (P = 0.3)	Not available
METABRIC		High	<i>Better</i> (P = 0.5)	Poor (P = 0.2)

\*Statistically significant

**Table 4.** Spearman correlation table between LSD1/*KDM1A* and key immune-response genes  
A) LSD1/LSD1-associated DEGs and immune-response genes in the SGH cohort

SGH cohort (Spearman's correlation test)							
	LSD1_Nuclear_Hscore	COP55	Eloc	MTDH	VEGFR1	CCL5	CXCL9
LSD1_Nuclear_Hscore	1.00	NA	NA	NA	NA	NA	NA
COP55	0.19	1.00	NA	NA	NA	NA	NA
Eloc	0.23	0.70	1.00	NA	NA	NA	NA
MTDH	0.16	0.60	0.53	1.00	NA	NA	NA
VEGFR1	0.33	0.18	0.35	0.03	1.00	NA	NA
CCL5	-0.04	-0.15	-0.18	-0.01	-0.08	1.00	NA
CXCL9	-0.03	-0.16	-0.14	0.02	-0.10	0.81	1.00
CXCL10	0.07	-0.03	0.11	0.04	0.14	0.72	0.65
CXCR3	-0.02	-0.18	-0.08	-0.02	0.03	0.72	0.74
CD3D	-0.04	-0.21	-0.19	-0.10	0.00	0.79	0.79
CD4	-0.02	-0.19	-0.12	-0.08	0.15	0.59	0.57
CD8A	-0.07	-0.21	-0.25	-0.07	-0.11	0.82	0.81
CD274	-0.06	-0.22	-0.18	-0.01	-0.07	0.65	0.63
IFNG	-0.08	-0.16	-0.25	-0.03	-0.20	0.55	0.60
	CXCL10	CXCR3	CD3D	CD4	CD8A	CD274	IFNG
LSD1_Nuclear_Hscore	NA	NA	NA	NA	NA	NA	NA
COP55	NA	NA	NA	NA	NA	NA	NA
Eloc	NA	NA	NA	NA	NA	NA	NA
MTDH	NA	NA	NA	NA	NA	NA	NA
VEGFR1	NA	NA	NA	NA	NA	NA	NA
CCL5	NA	NA	NA	NA	NA	NA	NA
CXCL9	NA	NA	NA	NA	NA	NA	NA
CXCL10	1.00	NA	NA	NA	NA	NA	NA
CXCR3	0.64	1.00	NA	NA	NA	NA	NA
CD3D	0.59	0.82	1.00	NA	NA	NA	NA
CD4	0.53	0.69	0.75	1.00	NA	NA	NA
CD8A	0.51	0.73	0.89	0.59	1.00	NA	NA
CD274	0.57	0.62	0.62	0.55	0.57	1.00	NA
IFNG	0.34	0.50	0.62	0.39	0.66	0.57	1.00







<b>CXCR3</b>	0.62	0.42	1.00	NA	NA	NA	NA	NA	NA	NA	NA	NA
<b>CD3D</b>	0.55	0.31	0.87	1.00	NA	NA	NA	NA	NA	NA	NA	NA
<b>CD3E</b>	0.47	0.31	0.76	0.81	1.00	NA	NA	NA	NA	NA	NA	NA
<b>CD3G</b>	0.52	0.28	0.75	0.87	0.76	1.00	NA	NA	NA	NA	NA	NA
<b>CD4</b>	0.32	0.23	0.67	0.70	0.79	0.64	1.00	NA	NA	NA	NA	NA
<b>CD8B</b>	0.34	0.13	0.59	0.74	0.60	0.71	0.54	1.00	NA	NA	NA	NA
<b>CD274</b>	0.60	0.46	0.61	0.63	0.53	0.64	0.51	0.40	1.00	NA	NA	NA
<b>IFNG</b>	0.72	0.40	0.63	0.66	0.54	0.65	0.45	0.60	0.79	1.00	NA	NA
<b>IFNGR1</b>	0.10	0.08	0.24	0.30	0.25	0.27	0.11	0.23	0.31	0.24	1.00	NA
<b>IFNGR2</b>	-0.16	-0.16	-0.17	-0.07	-0.16	-0.11	-0.17	-0.03	0.02	-0.09	0.36	1.00

## REFERENCES

1. Mehanna, J., et al., *Triple-negative breast cancer: current perspective on the evolving therapeutic landscape*. Int J Womens Health, 2019. **11**: p. 431-437.
2. Yin, L., et al., *Triple-negative breast cancer molecular subtyping and treatment progress*. Breast Cancer Res, 2020. **22**(1): p. 61.
3. Issa, J.P., *CpG island methylator phenotype in cancer*. Nat Rev Cancer, 2004. **4**(12): p. 988-93.
4. Basse, C. and M. Arock, *The increasing roles of epigenetics in breast cancer: Implications for pathogenicity, biomarkers, prevention and treatment*. Int J Cancer, 2015. **137**(12): p. 2785-94.
5. Kanwal, R., K. Gupta, and S. Gupta, *Cancer epigenetics: an introduction*. Methods Mol Biol, 2015. **1238**: p. 3-25.
6. Forneris, F., et al., *New roles of flavoproteins in molecular cell biology: histone demethylase LSD1 and chromatin*. Febs J, 2009. **276**(16): p. 4304-12.
7. Gu, F., et al., *Biological roles of LSD1 beyond its demethylase activity*. Cell Mol Life Sci, 2020. **77**(17): p. 3341-3350.
8. Lim, S., et al., *Lysine-specific demethylase 1 (LSD1) is highly expressed in ER-negative breast cancers and a biomarker predicting aggressive biology*. Carcinogenesis, 2010. **31**(3): p. 512-20.
9. Serce, N., et al., *Elevated expression of LSD1 (Lysine-specific demethylase 1) during tumour progression from pre-invasive to invasive ductal carcinoma of the breast*. BMC Clin Pathol, 2012. **12**: p. 13.
10. Nagasawa, S., et al., *LSD1 overexpression is associated with poor prognosis in basal-like breast cancer, and sensitivity to PARP inhibition*. PLoS One, 2015. **10**(2): p. e0118002.
11. Cao, C., et al., *Functional interaction of histone deacetylase 5 (HDAC5) and lysine-specific demethylase 1 (LSD1) promotes breast cancer progression*. Oncogene, 2017. **36**(1): p. 133-145.
12. Karakaidos, P., J. Verigos, and A. Magklara, *LSD1/KDM1A, a Gate-Keeper of Cancer Stemness and a Promising Therapeutic Target*. Cancers (Basel), 2019. **11**(12).
13. Zhou, M., et al., *KDM1A inhibition is effective in reducing stemness and treating triple negative breast cancer*. Breast Cancer Res Treat, 2021. **185**(2): p. 343-357.

14. Wang, T., F. Zhang, and F. Sun, *ORY-1001, a KDM1A inhibitor, inhibits proliferation, and promotes apoptosis of triple negative breast cancer cells by inactivating androgen receptor*. *Drug Dev Res*, 2022. **83**(1): p. 208-216.
15. Liu, Y., et al., *LSD1 inhibition sustains T cell invigoration with a durable response to PD-1 blockade*. *Nat Commun*, 2021. **12**(1): p. 6831.
16. Qin, Y., et al., *Inhibition of histone lysine-specific demethylase 1 elicits breast tumor immunity and enhances antitumor efficacy of immune checkpoint blockade*. *Oncogene*, 2019. **38**(3): p. 390-405.
17. Sheng, W., et al., *LSD1 Ablation Stimulates Anti-tumor Immunity and Enables Checkpoint Blockade*. *Cell*, 2018. **174**(3): p. 549-563.e19.
18. Thike, A.A., et al., *Loss of androgen receptor expression predicts early recurrence in triple-negative and basal-like breast cancer*. *Mod Pathol*, 2014. **27**(3): p. 352-60.
19. Yeong, J., et al., *Higher densities of Foxp3(+) regulatory T cells are associated with better prognosis in triple-negative breast cancer*. *Breast Cancer Res Treat*, 2017. **163**(1): p. 21-35.
20. Sherman, B.T., et al., *DAVID: a web server for functional enrichment analysis and functional annotation of gene lists (2021 update)*. *Nucleic Acids Res*, 2022. **50**(W1): p. W216-w221.
21. Huang da, W., B.T. Sherman, and R.A. Lempicki, *Systematic and integrative analysis of large gene lists using DAVID bioinformatics resources*. *Nat Protoc*, 2009. **4**(1): p. 44-57.
22. Szklarczyk, D., et al., *The STRING database in 2023: protein-protein association networks and functional enrichment analyses for any sequenced genome of interest*. *Nucleic Acids Res*, 2023. **51**(D1): p. D638-d646.
23. Shannon, P., et al., *Cytoscape: a software environment for integrated models of biomolecular interaction networks*. *Genome Res*, 2003. **13**(11): p. 2498-504.
24. Chin, C.H., et al., *cytoHubba: identifying hub objects and sub-networks from complex interactome*. *BMC Syst Biol*, 2014. **8 Suppl 4**(Suppl 4): p. S11.
25. Cerami, E., et al., *The cBio cancer genomics portal: an open platform for exploring multidimensional cancer genomics data*. *Cancer Discov*, 2012. **2**(5): p. 401-4.
26. Gao, J., et al., *Integrative analysis of complex cancer genomics and clinical profiles using the cBioPortal*. *Sci Signal*, 2013. **6**(269): p. p11.
27. Jiang, Y.Z., et al., *Genomic and Transcriptomic Landscape of Triple-Negative Breast Cancers: Subtypes and Treatment Strategies*. *Cancer Cell*, 2019. **35**(3): p. 428-440.e5.
28. Chen, Q., et al., *A comprehensive genomic and transcriptomic dataset of triple-negative breast cancers*. *Sci Data*, 2022. **9**(1): p. 587.
29. Scoumanne, A. and X. Chen, *The lysine-specific demethylase 1 is required for cell proliferation in both p53-dependent and -independent manners*. *J Biol Chem*, 2007. **282**(21): p. 15471-5.
30. Bradley, C., et al., *Carcinogen-induced histone alteration in normal human mammary epithelial cells*. *Carcinogenesis*, 2007. **28**(10): p. 2184-92.
31. Zhao, K., et al., *Comparison of the expression levels of lysine-specific demethylase 1 and survival outcomes between triple-negative and non-triple-negative breast cancer*. *Oncol Lett*, 2021. **21**(2): p. 102.
32. Devi, C.R., T.S. Tang, and M. Corbex, *Incidence and risk factors for breast cancer subtypes in three distinct South-East Asian ethnic groups: Chinese, Malay and natives of Sarawak, Malaysia*. *Int J Cancer*, 2012. **131**(12): p. 2869-77.
33. Tang, S., et al., *Differential outcomes in triple negative breast cancer observed among the major ethnic groups in Singapore*. *Clinical Practice*, 2019. **16**.

34. Telli, M.L., et al., *Asian ethnicity and breast cancer subtypes: a study from the California Cancer Registry*. *Breast Cancer Res Treat*, 2011. **127**(2): p. 471-8.
35. Cui, X., H. Zhu, and J. Huang, *Nomogram for Predicting Lymph Node Involvement in Triple-Negative Breast Cancer*. *Front Oncol*, 2020. **10**: p. 608334.
36. Wang, X.X., et al., *Effect of nodal status on clinical outcomes of triple-negative breast cancer: a population-based study using the SEER 18 database*. *Oncotarget*, 2016. **7**(29): p. 46636-46645.
37. Kumar, P. and R. Aggarwal, *An overview of triple-negative breast cancer*. *Arch Gynecol Obstet*, 2016. **293**(2): p. 247-69.
38. Burstein, M.D., et al., *Comprehensive genomic analysis identifies novel subtypes and targets of triple-negative breast cancer*. *Clin Cancer Res*, 2015. **21**(7): p. 1688-98.
39. Shi, Y.J., et al., *Regulation of LSD1 histone demethylase activity by its associated factors*. *Mol Cell*, 2005. **19**(6): p. 857-64.
40. Wang, S., et al., *MicroRNA-17 acts as a tumor chemosensitizer by targeting JAB1/CSN5 in triple-negative breast cancer*. *Cancer Lett*, 2019. **465**: p. 12-23.
41. Wang, L., et al., *Pan-cancer analyses of Jab1/COPS5 reveal oncogenic role and clinical outcome in human cancer*. *Heliyon*, 2022. **8**(12): p. e12553.
42. Brown, D.M. and E. Ruoslahti, *Metadherin, a cell surface protein in breast tumors that mediates lung metastasis*. *Cancer Cell*, 2004. **5**(4): p. 365-74.
43. Dhiman, G., et al., *Metadherin: A Therapeutic Target in Multiple Cancers*. *Front Oncol*, 2019. **9**: p. 349.
44. Malekian, S., et al., *Expression of Diverse Angiogenesis Factor in Different Stages of the 4T1 Tumor as a Mouse Model of Triple-Negative Breast Cancer*. *Adv Pharm Bull*, 2020. **10**(2): p. 323-328.
45. Nishitani, H. and Z. Lygerou, *Control of DNA replication licensing in a cell cycle*. *Genes Cells*, 2002. **7**(6): p. 523-34.
46. Wang, Y., et al., *LSD1 is required for euchromatic origin firing and replication timing*. *Signal Transduct Target Ther*, 2022. **7**(1): p. 102.
47. Mahadevappa, R., et al., *The prognostic significance of Cdc6 and Cdt1 in breast cancer*. *Sci Rep*, 2017. **7**(1): p. 985.
48. Ueda, A., et al., *Therapeutic potential of PLK1 inhibition in triple-negative breast cancer*. *Lab Invest*, 2019. **99**(9): p. 1275-1286.
49. de Cárcer, G., *The Mitotic Cancer Target Polo-Like Kinase 1: Oncogene or Tumor Suppressor?* *Genes (Basel)*, 2019. **10**(3).
50. Dalvi, P.S., et al., *LSD1 Inhibition Attenuates Tumor Growth by Disrupting PLK1 Mitotic Pathway*. *Mol Cancer Res*, 2019. **17**(6): p. 1326-1337.